THE UNIVERSITY OF MICHIGAN
RADIO ASTRONOMY OBSERVATORY

UM/RAO REPORT NO. 70-5

THE REDUCTION AND ANALYSIS OF DATA FROM THE LOW-FREQUENCY RADIO ASTRONOMY EXPERIMENT ABOARD THE OGO-IV SPACECRAFT

Final Report
NASA Contract NAS5-3099
NASA Grant NGR-23-005-371

Submitted by:
Fred T. Haddock
Project Director

July 1970

DEPARTMENT OF ASTRONOMY

UM/RAO REPORT NO. 70-5

THE REDUCTION AND ANALYSIS OF DATA FROM THE LOW-FREQUENCY RADIO ASTRONOMY EXPERIMENT ABOARD THE OGO-IV SPACECRAFT

Final Report
NASA Contract NAS5-3099
NASA Grant NGR-23-005-371

Submitted by:
Fred T. Haddock
Project Director

July 1970

Written by:
William H. Potter

RADIO ASTRONOMY OBSERVATORY
UNIVERSITY OF MICHIGAN
ANN ARBOR, MICHIGAN 48104

SUMMARY

The purpose of the OGO-IV radio astronomy experiment was to map the brightness temperature of the sky at a frequency of 2.5 MHz, using a short monopole antenna on the spacecraft, and depending upon the ionospheric focussing effect to achieve angular resolution. The experiment operated for the life of the spacecraft (7/67 - 10/69), returning data from radiometers operating at 2.0 and 2.5 MHz, respectively, and measurements of the complex impedance of the antenna at 2.5 MHz as the spacecraft passed up and down through the ionosphere.

Radio frequency interference generated within the spacecraft makes the interpretation of the radiometer data very difficult, and it appears to be impractical to extract mapping information. The antenna impedance measurements are not affected by the interference and represent a useful body of data for the study of the properties of the ionosphere, and the behavior of antennas in plasma.

In connection with the project, theoretical investigations have been carried out in such fields as the behavior of antennas in plasma, and the propagation of electro-magnetic waves in plasma.

TABLE OF CONTENTS

LIST OF FIGURES

I. INTRODUCTION

This is the final scientific report on the University of Michigan Radio Astronomy experiment carried aboard the OGO-IV spacecraft. The OGO-IV experiment was essentially identical with the earlier experiment carried aboard OGO-II, and the two have been developed, operated, and the data analyzed under contract NAS5-3099, from Goddard Space Flight Center, NASA, and grant NGR-23-005-371, from NASA Headquarters. Most of the data reduction effort, as well as the engineering of the flight instrument, was supported under the contract. Work done under the grant has consisted largely of review and re-assessment of the method of scientific analysis, in an effort to find a satisfactory way of extracting mapping information.

The Radio Astronomy Observatory of the University of Michigan has carried out an extensive program of low frequency observations from spacecraft. Measurements of the integrated brightness temperature of the celestial sphere were made from rockets, and low frequency radiometers have been carried aboard each of the first five of the OGO-series spacecraft. Three of these, carried on OGO's I, III, and V, were designed primarily to study the low frequency components of solar radio bursts. Two, aboard OGO's II and IV, were designed to utilize the focusing effect of the ionosphere to obtain low-resolution maps of the low-frequency brightness temperature of the celestial sphere.

Except for OGO-I, the solar burst experiments have been quite successful. The mapping experiments have encountered various problems, the most serious of which was the extremely high radio noise level encountered on both spacecraft. It became obvious quite early that no mapping information could

be extracted from the OGO-II data, because of the high noise level, the failure of the spacecraft to stabilize, and the high orbit of OGO-II (Potter, 1968). It has been possible, however, to utilize OGO-II data to study the wake produced by the spacecraft as it moves through the ionosphere, an unexpected benefit (Yorks, Weil, and Potter, 1968, Yorks and Weil, 1970).

OGO-IV experienced a lower noise level than OGO-II, but higher than either OGO-III or V. It was obvious that this noise level would make it difficult to extract useful mapping information. Subsequent analysis has shown that it is indeed extremely difficult to extract mapping information, and probably impossible to do so. The large body of experiment data should, however, be useful in analyzing the properties of the ionosphere, and the behavior of the radio antennas in it.

Chapter II of this report covers the scientific background for the experiment. It includes discussions of the state of the art of low-frequency radio astronomy, the theory of ionospheric focusing, upon which the mapping experiment depends, and a discussion of the behavior of antennas in a plasma, such as the ionosphere.

Chapter III describes briefly the experiment, the spacecraft, and their history. A more complete report on this topic is the OGO-IV Final Engineering Report (Yorks and Cohen, 1969).

Chapter IV describes the methods developed for the analysis of the data, the various kinds of data collected by the experiment, and the forms in which the data now exist.

Chapter V summarizes the conclusions which may be drawn from the OGO-IV experience.

II. BACKGROUND

A. LOW-FREQUENCY RADIO ASTRONOMY

The portion of the radio spectrum which is observable from the surface of the earth extends from roughly five or ten MHz to a few hundred GHz. Higher frequencies are cut off by molecular absorption in the atmosphere, and lower frequencies by free electrons in the ionosphere. Frequencies of a few MHz and below can be observed only from rockets and spacecraft above the f-layer of the ionosphere, at heights at least a few hundred kilometers above the earth's surface.

Radio astronomy observations at frequencies below the ionospheric cutoff are important for several reasons, mostly deriving from the fact that the generation, propagation, and absorption of these frequencies are strongly affected by the presence of free electrons. Low-frequency observations can give information about regions too tenuous, and events too violent, to be studied in any other way. Since electrons of different energies interact with magnetic fields in different ways, we can often determine the magnetic field strength and/or the electron energy. Thus low-frequencies are a useful probe to study such diverse regions as the solar corona, the interplanetary medium, the interstellar medium, and the various types of radio sources where synchrotron emission takes place, such as supernova remnants, radio galaxies, and quasars.

1. Radio Spectra

Most radio sources show very simple spectra, and fall into one of two classes: (1) the "thermal" sources, with black-body spectra, and (2) the "non-thermal" sources whose spectra can

be described by the power law

$$S = k\ \nu^{\alpha}\ , \qquad \text{(II-1)}$$

where S is the flux density, k a factor of proportionality, ν the frequency of observation, and α is the parameter of the source, called the spectral index. The interest of low-frequency astronomers is confined primarily to the non-thermal sources.

Non-thermal sources are a heterogeneous group of objects, and include quasars, pulsars, supernova remnants, radio galaxies, and normal galaxies (including our own). The common property of these objects is that their emission is believed to be synchrotron radiation, generated by relativistic electrons in a magnetic field. These objects include some of the most puzzling in the universe, and any observations which illuminate their nature are important.

For many of the non-thermal sources, the spectral index, α, lies between -0.5 and -1.0 over the range of frequencies presently observed. Thus Equation (II-1) indicates that the flux increases toward lower frequencies without limit, an obvious impossibility, first, because the source itself must have a low-frequency cutoff, and second, because the radiation must propagate through a medium which has a low-frequency cutoff. Determination of the frequency of maximum flux, f_{max}, and of α at frequencies below f_{max} should tell us something of the nature of the source, the intervening medium, or both.

The theory of synchrotron emission, as developed in recent years (see Scheuer and Williams, 1968, for a review of radio spectra) indicates that the intrinsic spectrum of a source should show a maximum at about the frequency at which the source becomes optically thick. Above f_{max}, α should be a function of the energy distribution of the electrons, among

other things. Below f_{max}, α depends upon the absorption mechanism. Some studies indicate that α should be about 2.5, if synchrotron self-absorption is the dominant mechanism. Any absorption between the emitting region and the observer, whether it be a part of the source or of the intervening medium may be expected to show a different slope below f_{max}. Hence measurement of this slope will tell us whether the spectrum we see is that of the synchrotron emitter itself, or has been distorted by other absorption mechanisms. The information is valuable, in either case.

There are few radio sources for which f_{max} and α below f_{max} have been well observed. There are spectra which show evidence of a turn-down, but generally this evidence consists of one point, which cannot define the slope below f_{max}. A few sources with irregular spectra show secondary maxima at high frequencies, which are generally attributed to very compact clouds of high energy electrons, within a larger source. These spectra are shown to be variable on a time scale of months, indicating that dynamic processes must be taken into account in explaining them. In any event, they seem always to be superposed upon a power law spectrum whose f_{max} is in the unobserved region. Because of these complications, no one has yet succeeded in interpreting the irregular spectra with confidence, though theoretical treatments exist for simplified models (van der Laan 1966, MacCray 1969). The interpretation of the simpler synchrotron spectra of the "standard" non-variable sources should be a much simpler problem, if only the observational data could be extended toward lower frequencies far enough to reveal f_{max} and α below f_{max}.

2. Observations from the Earth's Surface

Terrestrial radio telescopes can reliably observe only at frequencies that are substantially above the critical frequency of the ionosphere (the plasma frequency at the level of maximum electron density in the f-layer) at the time and place of the observations. Frequencies below the critical frequency are not propagated at all, and frequencies near the critical frequency are subject to uncertainties due to absorption and scintillation in the ionosphere.

The critical frequency varies with the time of day, time of year, geographic location, the eleven year solar cycle, and with other non-periodic parameters. The lowest values tend to occur during winter nights near sunspot minimum, at locations of moderately high geo-magnetic latitude. Under favorable conditions, the critical frequency will usually be below ten MHz, and may rarely go as low as one MHz. Under unfavorable conditions, values larger than 30 MHz are not unusual.

Several observers have demonstrated the feasibility of making useful observations from the earth's surface at 10 MHz and below. For example, Bridle and Purton (1968) cataloged 124 sources at 10.03 MHz, with a resolution of better than 3° in both directions. Ellis and others in Tasmania (Ellis, 1957, 1965; Ellis and Hamilton, 1964, 1966; Ellis, Waterworth, and Bessel 1962) report scans across the galactic plane at frequencies as low as 1.6 MHz and a partial survey at 4.7 MHz with a resolution of 11° by 3°, in which a few sources were isolated. Ellis and Hamilton (1966) publish spectra of four sources, using their data at 4.7 MHz, and other observations at higher frequencies. These spectra show evidence of turning down below 10 MHz, but the points are far too few to determine the slope of f_{max}.

Ground observations at low frequencies have, of course, been impossible during the current period of high solar activity. Presumably, low-frequency work will be resumed as the solar activity declines, so that we may expect new data to appear in a few years. It is important to be aware of the limitations of ground observations at low frequencies, however, so that we do not expect too much. Some of these limitations are:

1. The absolute lower limit in frequency appears to be about 1.5 MHz. Even the most optimistic workers do not expect to reach lower frequencies. Any work below 3 or 4 MHz will consist of scattered observations. Observations at least as low as 1 MHz have been required to establish the low-frequency slope of the integrated cosmic background. We expect that the spectra of several sources must be known in this region if we are to determine whether the low-frequency slopes of individual sources differ from the average.

2. The correlation of the critical frequency with both time of day and time of year means that there is an observationl selection effect in right ascension, as well as declination. For observatories in the southern hemisphere, the favored region includes the galactic center. For northern observatories, it is diametrically opposite. This correlation makes impossible any homogeneous survey of the sky.

3. The correlation of favorable observing conditions with the level of solar activity presents difficulties in interpreting any observations of phenomena which might be related to solar activity. Obviously, observations of the sun become impossible at the time when they become most interesting. Changes in the emission of Jupiter with the level of solar activity might be masked, as would be changes in the low-

frequency absorption of the interplanetary medium.

4. The restriction to observing on winter nights during sunspot minimum means that any variable sources with periods of the order of either one year or eleven years would not be detected.

It is interesting to speculate on what might be achieved in low-frequency radio astronomy from the ground during the next sunspot minimum, if a vigorous program were undertaken. It should be noted that no such program is getting under way in this country, at least.

We might expect fairly complete, though not uniform, surveys of the entire sky at about 10 MHz, with a resolution of perhaps 1°.

Fluxes of perhaps 100 sources might be measured with usable accuracy at about 5 MHz, and one or two dozen at 3 MHz. At 5 MHz, surveys of discrete sources might be reasonably complete to about 200 flux units, over perhaps 25% of the sky.

Maps of the flux distribution at 5 MHz might cover half the sky, at a resolution of the order of 3°.

Scattered observations will continue at frequencies below 3 MHz, including scans across the galactic plane, and other regions of special interest.

3. Low-Frequency Observations from Space

Directivity, rather than sensitivity, is the limiting factor in low-frequency radio astronomy from space. A simple radiometer, using an antenna ten to twenty meters in length orbiting in a radio-quiet spacecraft, can reach the cosmic background. However, directivity of any kind is difficult to attain. To date, no observational data have been published (with the possible exception of RAE) with an angular resolution

much better than a hemisphere. A structure whose dimensions are measured in hundreds of meters is required to achieve significantly better resolution.

Certain researches do not require directivity. Solar radio bursts are sufficiently strong and sufficiently unique in form that they may readily be identified and measured by non-directional instruments. The integrated cosmic background, by definition, is that which is measured by a non-directional instrument. The sources contributing to the cosmic background are sufficiently heterogeneous, however, that only limited conclusions can be drawn from their integrated radiation.

For observations other than these, some directivity is required to separate one source from another. An angular resolution of a few degrees would permit several sources to be identified. Increasing resolution would isolate more sources, seemingly without limit. Even surveys of radio sources made at higher frequencies with instruments of excellent resolution tend to be limited more by resolution than sensitivity.

Except for the ionospheric focussing method, directivity can be attained only from an antenna structure which is large compared with the wavelength of observation. Several methods have been proposed for erecting such structures in orbit. Rhombic and vee antennas may be composed of either rigid or flexible conductors. Arrays of dipoles may be connected by rigid links or flexible tethers, or they may be "flown in formation" by small rockets, without mechanical connections. Aperture synthesis methods may be used, requiring only a few antenna elements.

The Radio Astronomy Explorer (Alexander, et. al., 1969) appears to be the only attempt to date to orbit a directional antenna for low frequencies. The antenna consists of a pair of semi-rigid vee's with legs 229 m long. Radiometers are

provided to cover the frequency range from 0.2 to 9.18 MHz. Obviously, the directivity at the lowest frequencies is vanishingly small, but at higher frequencies the RAE may provide spectral data with sufficent angular resolution to distinguish different parts of the galaxy. It should also provide an interesting supplement to the partial maps of low-frequency radiation obtained by Ellis and his associates in Tasmania (Ellis and Hamilton, 1966). The RAE data should eventually provide a more complete coverage of the sky than the ground observations, but will not approach the resolution.

Proposals have been made for orbiting larger antenna arrays, capable of resolving several discrete sources. A study (Haddock, 1966) has indicated the feasibility of a rhombic array capable of resolving several sources at 1 MHz. Frequencies at least this low appear to be required to determine the nature of the low frequency cutoff in various sources. However, there does not appear to be any such instrument under construction.

4. Ionsopheric Focussing Experiment

The ionospheric focussing experiment was first proposed in 1962 (Haddock, 1962a, 1962b). At that time, few radio astronomy observations of any kind had been made at frequencies below 20 MHz. The objective of the OGO-IV experiment was to map the celestial sphere at a frequency of 2.5 MHz, with a resolution of the order of 20°. In the intervening years, many low-frequency programs have been carried out, but the basic objective of the OGO-IV experiment remains elusive. Ground observations have achieved better resolution, but only at higher frequencies, and without complete and homogeneous coverage. The Radio Astronomy Explorer may exceed the 20° resolution figure at higher frequencies, but at 2.5 MHz, its

antenna elements are only 1.9 wavelengths long, so it is unlikely that its resolution will approach 20°.

The OGO-IV experience has failed to demonstrate the practicality of the ionosphere focussing method, but, on the other hand, it has not revealed any immovable obstacles. An ionospheric focussing experiment, if flown in a suitable spacecraft, still appears feasible, and is the only alternative to orbiting a large structure, if the low-frequency portion of the spectrum is to be adequately observed.

B. IONOSPHERIC FOCUSSING

1. General

An isotropic antenna located in the upper ionosphere at a level just above the cutoff level for the operating frequency, will not receive radiation from the entire himisphere, but only from a roughly circular region surroundind the local zenith, whose angular diameter decreases to zero as the antenna approaches the critical level for that frequency. This is the so called ionospheric focussing effect, upon which the OGO-IV mapping experiment is based.

The theory of ionospheric focussing has been developed rather extensively as a necessary background to the interpretation of the OGO-IV data, and the final form of the theory has been published by Walsh and Weil (1968). They derive analytic expressions for the antenna gain as a function of angular position, neglecting only the effect of collisions and radiometer bandwidth. The effect of the magnetic field and the contribution of the gain pattern of the antenna itself are included. In general, the effective antenna gain pattern, as projected on the celestial sphere, is circular or elliptical, with a high effective gain near the edges,

and a somewhat reduced gain in the center. The elongation of the elliptical patterns is a function of the magnetic field, and the distribution of gain within the pattern is dependent upon the magnetic field and its orientation, and upon the gain pattern of the antenna itself. For zero bandwidth and zero collision frequency, as assumed by Walsh and Weil, the gain at the edge of the pattern is infinite. However, both of these effects tend to smear the edges of the pattern, removing the infinity.

2. Simple Theory

While the theory of ionsopheric focussing presented by Walsh and Weil (1968) is general and complete, it is not very convenient for illustrative purposes. The numerical calculations are lengthy, and the results are expressed as antenna gain as a function of angular coordinates. Thus beam width may not be readily deduced without computing gain at many points. We shall develop here a simple theory which gives the beamwidth directly for both modes of propagation, and which is exact under conditions of a passage through the ionosphere near the earth's equator. The theory is based upon applying Snell's law to relate the angle of total reflection to the local index of refraction, and evaluating the index of refraction from a simplified form of the Appleton-Hartree formula.

a. Snell's Law

When radiation passes from a medium whose refractive index is unity (free space) to an isotropic medium whose refractive index is n, its angle of incidence (with respect to the direction of the gradient of n) changes according to Snell's law:

$$\sin i_2 = \frac{1}{n} \sin i_1 \qquad \text{(II-2)}$$

In an ionized medium, such as the ionosphere, the refractive index is generally less than 1. Thus for certain values of n and i_1,

$$\frac{1}{n} \sin i_1 > 1,$$

and the radiation cannot be refracted, but instead it experiences "total internal reflection." Thus the condition:

$$\frac{1}{n} \sin i_1 = 1$$

marks the lowest level in the ionosphere to which radiation incident at i can penetrate, and also marks the greatest angle of incidence which radiation may have and still penetrate to a given level in the ionosphere. Specifically

$$\sin i_c = n, \qquad \text{(II-3)}$$

where i_c is the greatest angle of incidence. Obviously, an isotropic antenna located at a level whose refractive index is n will receive radiation only from a cone of half-angle i_c, centered on the zenith. If the antenna descends into the ionosphere so that $n \to 0$, then $i_c \to 0$, and the beam narrows, only to disappear entirely at $n = 0$. No radiation from outside the ionosphere can penetrate below this level.

The refractive index at any point in the upper ionosphere may be found from the Appleton-Hartree formula, discussed below. In general, n is complex, multi-valued, and non-iostropic. Walsh and Weil (1968) have treated the multivalued, non-isotropic case, and have shown that in the region where OGO-IV focussing takes place, the collision frequency is small, hence the imaginary terms in n are negligible. In the treatment below, we present an approximation which is multi-valued, but isotropic.

b. Appleton-Hartree Formula

The general Appleton-Hartree (A-H) formula for refractive index in a magneto-ionic medium is:

$$n^2 = 1 - \frac{X}{1 - iZ - \frac{Y^2 \sin^2\theta}{2(1-X-iZ)} \pm \left(\frac{Y^4 \sin^4\theta}{4(1-X-iZ)^2} + Y^2 \cos^2\theta \right)^{1/2}} \qquad \text{(II-4)}$$

where

$X = f_p^2/f^2 =$ (plasma freq.)^2/(operating freq.)^2

$Y = f_g/f =$ (electron gyro freq.)/(operating freq.)

$Z = f_c/f =$ (electron collision freq.)/(operating freq.)

$\theta =$ Angle between magnetic field and wave normal.

If Z is vanishingly small, we may neglect all the imaginary terms, and write (as do Walsh and Weil, 1968):

$$n^2 = 1 - \frac{X}{1 - \eta Y}, \text{ where} \qquad \text{(II-5)}$$

$$\eta = \frac{Y \sin^2\theta}{2(1-X)} \pm \left(\frac{Y^2 \sin^4\theta}{4(1-X)^2} + \cos^2\theta \right)^{1/2} \qquad \text{(II-6)}$$

Note, however, that to neglect terms i Z, we must have

$$|Z| \ll 1, \text{ and } |Z| \ll (1-X).$$

The latter condition is somewhat troublesome, since later we will be concerned with what happens as $X \to 1$. By convention, the value derived from the upper sign: the + sign in (II-4) and the - sign in (II-6), refers to the "ordinary mode" (O-mode), and

the lower sign refers to the "extra-ordinary mode" (E-mode). If $Y = 0$, indicating no magnetic field, then the two modes converge. If $Y > 0$, the two modes diverge, and the medium is bi-refringent. We shall show below that the reflection level for the 0-mode, but not the index of refraction, is independent of the magnetic field, while that of the E-mode is dependent upon the magnetic field.

c. Reflection Levels

The A-H formula may be solved directly to determine the levels in the ionosphere where $n=0$, which represent reflection levels, through which radiation cannot pass. The regions just above the reflection levels are the focussing regions.

We may set $n = 0$ in (II-5), and solve for X, obtaining:

$$X = 1,$$
$$X = 1 \pm Y.$$

The solution $X = 1$, which is identical to that obtained when $Y = 0$, is the reflection level for the "ordinary mode" of propagation in the bi-refringent medium. The solution $X = 1 - Y$ is the reflection level for the extra-ordinary mode of propagation. The solution $X = 1 + Y$ represents a reflection level to which radiation originating outside the ionosphere will never penetrate, because, to reach this level, it must pass through both $X = 1$ and $X = 1 - Y$. It may play a role in reflecting radiation which is produced within the ionosphere, though.

We should expect, then, a focussing region for the extra-ordinary mode just above the level where $X = 1 - Y$, and another for the ordinary mode just above the level where $X = 1$. These results indicate that the location of the reflection levels for both modes are independent of θ. The reflection level for the E-mode depends on the magnitude, but not on the direction, of the magnetic field. Thus the ionosphere acts as an isotropic medium at the reflection level, but not necessarily in the focussing region just above it.

d. Approximation to A-H Formulas

For a simple theory of focussing, we wish to make use of Equation (II-3) to determine the effective beamwidth, using the A-H formula to evaluate n. However, for (II-3) to be valid, n must be independent of θ, and the A-H formula in the form of (II-5) and (II-6) contains θ. We need an approximation which is independent of θ. There are three special cases of the A-H formula that are commonly developed as approximations: (1) the case of zero magnetic field (Y=0), (2) the case of quasi-longitudinal propagation (QL), and (3) the case of quasi-transverse propagation (QT).

If Y = 0, the A-H forumla reduces to :

$$n^2 = 1 - X. \qquad \text{(II-7)}$$

Obviously, $n \to 0$ as $X \to 1$, hence i_c, the half-angle of the effective beam, approaches 0 also, vanishing when X = 1. However, for typical OGO-IV orbits, $0.2 < Y < 0.4$. Since η may be quite large, we can hardly assume that ηY vanishes.

The QL and QT approximations derive from letting one or the other of the two terms under the radical in (II-6) vanish. QL conditions apply if the term in sin θ is negligible, as it will be if $\theta = 0$ (propagation along the magnetic field), if Y is small, or if X becomes very large. QT conditions apply if the term in cos θ is negligible, as it will be if $\theta = 90°$ (propagation perpendicular to the magnetic field), or if $X \to 1$ for intermediate values of θ.

For typical OGO-IV passes, QT conditions are more appropriate than QL. Since $0.2 < Y < 0.4$ and X is never very large, the sine term in (II-6) can be neglected only if θ is very close to 0. On the other hand, when X approaches 1, the sine term becomes much larger than the cosine term over a substantial range of θ. Thus QT conditions hold over a greater range of θ than QL, especially in the focussing region for the ordinary mode.

Furthermore, for passes near the magnetic equator, where the magnetic field is horizontal, the assumption that $\theta = 90°$ is valid for all rays which come to focus in a plane perpendicular to the magnetic field. Thus for focussing in this plane, the QT condition is satisfied. There is no corresponding plane in which $\theta = 0°$ for all rays.

e. Approximations to n Based on QT Conditions

The QT assumption may be used in several different ways to derive different approximations to the A-H formula. We may:

1. Set $\theta = 90°$.
2. Set $\sin\theta = 1$, but retain $\cos\theta$.
3. Set $\cos\theta = 0$, but retain $\sin\theta$.
4. Expand the radical using the binomial theorem, assuming the sine term larger than the cos term.

Of these, only the first yields an expression for n that is independent of θ, and therefore is directly useful for our purpose. The others are useful only to evaluate the error introduced in the expression derived from 1 when θ departs from 90°, and to illustrate the general intractibility of the A-H formula.

Approximation 1: $\theta = 90°$.

We obtain:

$$\eta = \frac{Y}{2(1-X)} \pm \left(\frac{Y^2}{4(1-Y)^2} \right)^{1/2}$$

Using the - sign for the 0-mode,

$$\eta = 0$$

$$n^2 = 1-X \qquad \text{(II-8)}$$

Using the + sign for the E-mode,

$$\eta = \frac{Y}{1-X}$$

$$n^2 = 1 - \frac{X}{1 - \frac{Y^2}{1-X}} = \frac{(1-X)^2 - Y^2}{(1-X) - Y^2} \qquad \text{(II-9)}$$

Approximation 2: Sin θ = 1.

This approximation would be justified if θ departs somewhat from 90°, and $Y^2/4(1-X)^2$ is of the order of 1, or smaller.

$$\eta = \frac{Y}{2(1-X)} \pm \left(\frac{Y^2}{4(1-X)^2} + \cos^2 \theta \right)^{1/2}$$

$$n^2 = 1 - \frac{2X\ (1-X)}{2(1-X) - Y^2 \pm (Y^4 + 4(1-X)^2\ Y^2 \cos^2 \theta)^{1/2}} \qquad \text{(II-10)}$$

This form seems to offer little useful simplification, as compared with the complete formula.

Approximation 3: Cos θ = 0.

This approximation would be justified if θ departs somewhat from 90°, and $Y^2/4(1-X)^2 >> 1$.

$$\eta = \frac{Y \sin^2 \theta}{2(1-X)} \pm \left(\frac{Y^2 \sin^4 \theta}{4(1-X)^2} \right)^{1/2}$$

For the 0-mode, use the - sign:

$$n^2 = 1 - X \qquad \text{(II-11)}$$

For the E-mode, use the + sign:

$$n^2 = 1 - \frac{X}{1 - \frac{Y^2 \sin^2\theta}{1-X}} = \frac{(1-X)^2 - Y^2 \sin^2\theta}{(1-X) - Y^2 \sin^2\theta} \qquad \text{(II-12)}$$

These expressions are identical with those from Approx. 1, except for the $\sin^2\theta$ terms in the E-mode. They must be used with care, since they say that, for the E-mode, n = 0 at X = 1-Y sin θ, while we have already shown that n = 0 at X = 1 - Y for all θ.

Approximation 4: Binomial Expansion.

Using the QT assumption that

$$\frac{Y^2 \sin^4\theta}{4(1-X)^2} >> \cos^2\theta, \qquad \text{(II-13)}$$

we may expand the quantity under the radical by the binomial theorem. We will get an expression for n containing an infinite series, of which we can keep as many terms as desired. This approach would seem to offer a better approximation than any of the preceeding. Unfortunately, it produces some peculiar results.

If a > b, the binomial theorem yields:

$$(a+b)^{1/2} = a^{1/2} + \frac{1}{2} a^{-1/2} b - \frac{1}{8} a^{-3/2} b^2 + \frac{1}{16} a^{-5/2} b^3 \ldots$$

Substitute

$$a = \frac{Y^2 \sin^4\theta}{4(1-X)^2}, \quad b = \cos^2\theta.$$

$$\eta = \frac{Y \sin^2\theta}{2(1-X)} \pm \frac{Y \sin^2\theta}{2(1-X)} + \frac{(1-X)}{Y} \frac{\cos^2\theta}{\sin^2\theta} - \frac{(1-X)^3}{Y^3} \frac{\cos^4\theta}{\sin^6\theta} + \ldots$$

(II-14)

For the 0-mode, use the - sign:

$$\eta = -\frac{(1-X)}{Y}\cos^2\theta + \frac{(1-X)^3}{Y^3}\frac{\cos^4\theta}{\sin^6\theta} - \ldots$$

$$n^2 = 1 - \frac{X}{1 + (1-X)\cot^2\theta - \frac{(1-X)^3}{Y^2}\frac{\cos^4\theta}{\sin^6\theta} + \ldots}$$

(II-15)

The term $(1-X)\cot^2\theta$ is peculiar, because one would not expect to encounter a term which depends upon the direction of the magnetic field, but not on its magnitude. Note, however, that the QT assumption fails as Y approaches 0, so we do not expect this expression to hold for small Y, although perhaps it is a valid approximation for a certain range of Y. It does have the encouraging property that $n \to 0$ as $X \to 1$.

For the E-mode, we use the + sign, obtaining

$$n^2 = 1 - \frac{X}{1 - \frac{Y^2\sin^2\theta}{(1-X)} - (1-X)\cot^2\theta + \frac{(1-X)^3}{Y^2}\frac{\cos^4\theta}{\sin^6\theta} + \ldots}$$

(II-16)

The first two terms in the denominator are the same as those obtained from Approximation 3. Again, however, we have the troublesome term $(1-X)\cot^2\theta$, which is more significant here than for the 0-mode, because we are interested in the 0-mode as $X \to 1$, but in the E-mode as $X \to 1 - Y$. Thus the cot term is larger in the E-mode focussing region than in the 0-mode region.

f. Summary of Simple Theory of Ionsopheric Focussing

Let us now assess these approximations to choose the best one for the 0-mode and E-mode focussing regions, respectively. For the 0-mode, Approximation 2 is not applicable, since in the 0-mode focussing region, X- 1 becomes very small. The other three approximations should hold. Approximations 1 and 3 give identical results, and Approximation 4, the binomial expansion, approaches the same result if either X-1 goes to zero, or cos θ goes to zero. Thus we may use the approximation

$$n^2 = 1 - X, \qquad \text{(II-7)}$$

with some confidence that it will hold over the 0-mode focussing region.

For the E-mode, only Approximation 1 yields an expression independent of θ, which we must use:

$$n^2 = \frac{(1-X)^2 - Y^2}{(1-X - Y^2} \; . \qquad \text{(II-9)}$$

The other approximations are useful only to estimate the range of θ over which (II-9) is valid.

At the E-mode reflection level, Y = 1-X. Hence the expression Y/2 (1-X), which determines the validity of Approximations 2 and 3, must be 1/2. Clearly, then, Approximation 3 is no longer applicable. Approximation 2 should be valid, but yields an expression hardly simpler than the full A-H formula. Furthermore, the series obtained from Approximation 4, the binomial expansion, will not converge very rapidly, except for θ very close to 90°.

Thus (II-9) represents the best isotropic approximation to n that we can derive for the E-mode, and it may be expected to hold over a small range of θ. Hence any beam widths derived using (II-9) will be applicable only for rays which are brought to a focus in a plane very nearly perpendicular to the magnetic field.

3. Beam Widths for Actual OGO-IV Passages

Using the simple theory of ionospheric focussing, and data from selected passages through the ionosphere, we can compute the approximate beam widths as a function of time. The results of such a calculation are presented in figure 1. The observational data upon which these curves are based are presented in Appendix A. The beam widths presented here correspond to the short axis of the elliptical beam predicted by the complete theory (Walsh and Weil, 1968). Beam widths have been computed for both modes of propagation, and for both of the OGO-IV radiometer frequencies, even though only the E-mode for 2.5 MHz is used in the OGO-IV experiment.

Figure 1 illustrates the time sequence of events, as the S/C moves down through the ionosphere. The differences between the two passages are attributable to the differences in magnetic field. For GI 3. the magnetic field is about 1.5 times stronger than for GI 8. Hence the E-mode has diverged farther from the O-mode. If the field were stronger yet, the 2.5 MHz E-mode cutoff would move earlier than the 2.0 MHz O-mode cutoff.

The extreme rapidity with which the beam converges is well illustrated in Figure 1. The E-mode converges from a half-width of 10° to 0° in less than 0.1 minute. Thus a

short integration time and a high sampling rate are required for an ionospheric focussing experiment to achieve a narrow effective beam.

In the OGO-IV experiment, the integration time is 0.5 sec, and the sampling period approximately 0.25 sec. There are effectively 12 independent samples taken during the time when the beam in converging from 10° half angle to zero. Thus we may say that there is an uncertainty in beam width due to the time constant which is of the order of <1°, which may safely be neglected.

4. Effect of Collisions on Ionospheric Focussing

The complete Appleton-Hartree formula for refractive index, Eq. II-4, includes terms in Z, the normalized collision frequency, as well as X and Y. As noted above (section IIB-2b), Z may be neglected only if $|Z| << 1$, and also $|Z| << |1-X|$. In both focussing regions, the latter condition is the more stringent of the two, since 1-X is always less than 1. In the 0-mode focussing, $X-1 \rightarrow 0$. Hence we can not neglect Z unless $Z \rightarrow 0$. In the E-mode region, $(X-1) \rightarrow Y$. For OGO-IV orbits, Y ranges from 0.2 to 0.3. For OGO-IV parameters, Z is of the order of 10^{-5}, and is negligible for focussing in either mode, though the margin of safety is somewhat greater for the E-mode.

The problem is greatly simplified by the fact that collisions may be neglected. If X is significant, the refractive index becomes complex, and the medium becomes absorbent, as well as refracting. The calculation of antenna impedance becomes more difficult, also.

5. Effect of Radiometer Bandwidth on Ionospheric Focussing

Our earlier work on ionospheric focussing has tended to neglect the defocussing effect of the finite bandwidth of the radiometer, particularly in the E-mode, which is the focussing mode used in the OGO-IV experiment. An approximation by Walsh (1961) evaluates the effect only for the 0-mode. The treatment of Walsh and Weil (1968) is general, in that their theory gives the gain distribution over the celestial sphere for both modes, and for any frequency. However, their numerical examples deal only with the 0-mode, and with monochromatic radiation. The Walsh and Weil theory could be used to determine the variation of beamwidth with frequency, but the computations are lengthy and laborious. Instead, we present calculations of the E-mode beamwidth as a function of frequency, based on the simpler expressions derived above.

The results of these calculations show that the E-mode focussing is somewhat more sensitive to bandwidth defocussing than the 0-mode, the defocussing increasing with the strength of the magnetic field. For typical conditions encountered in OGO-IV, the E-mode is defocussed by about 1.5 times as much as the 0-mode. Bandwidth defocussing will limit the best resolution attainable by OGO-IV to about 20 to 30° between half-power points.

The beamwidth has been calculated, using Snell's law and the Appleton-Hartree formula, subject to the assumptions:

(1) Collisions may be neglected.

(2) The magnetic field is everywhere perpendicular to the direction of propagation of the wave.

Assumption (1) is valid for OGO-IV conditions, particularly for E-mode focussing, as discussed in Section 4, above. Assumption (2) means that the treatment is valid only for focussing which occurs in a plane perpendicular to the earth's magnetic field. Thus it is applicable for passages near the equator, where the earth's magnetic field is horizontal, for determining the beamwidth in the east-west direction. These conditions happen to be those under which the narrowest beam is produced, so we are evaluating the best resolution which may be attained by the experiment. We must use the 0-mode examples of Walsh and Weil (1968) to estimate the relative beamwidth in other planes, and under conditions other than horizontal field.

Equations (II-7) and (II-9) are used to evaluate the index of refraction for the 0- and E-mode, respectively, and the beam width determined by

$$\theta = 2 \sin^{-1} n.$$

Figures 2, 3 and 4 are plots of calculated beamwidth as a function of plasma frequency, f_p. Curves are plotted for both the upper and lower frequency limit of the radiometer, for two values of gyro frequency, f_g, corresponding to values encountered during the actual passages labled GI 3 and GI 8 for both modes of focussing. It is significant to note that when the lower frequency band edge of the radiometer (2.47 MHz) is at the E-mode reflection level, the upper band edge sees an effective beam of 35 and 37°, respectively, for the two values of f_g.

C. ANTENNA IMPEDANCE IN A PLASMA

The characteristic impedance of an antenna may be affected by the presence of free electrons in its vicinity. Since ionospheric focussing takes place in a region of the ionosphere where free electrons strongly affect the index of refraction, it follows that they also strongly affect the impedance of the antenna. Further, the antenna impedance changes rapidly in the focussing region.

Radiometer data cannot be interpreted without knowledge of the antenna impedance. The quantity measured by a radiometer is a mean square of the noise voltage appearing across the input impedance of the radiometer, which is given by:

$$V_L^2 = 4\ kB\ T_A\ R_A \left| \frac{Z_L}{Z_A + Z_L} \right|^2 \qquad \text{(II-16)}$$

where:

- k = Boltzman's constant
- B = The radiometer bandwidth
- T_A = The antenna temperature
- R_A = The resistive component of the antenna impedance
- Z_A = The complex antenna impedance
- Z_L = The complex impedance of the radiometer input.

In order to deduce T_A from V_L, we must know both R_A and the quantity within the absolute magnitude signs, which accounts for the impedance match between the antenna and the radiometer. The OGO-IV experiment is capable of measuring the complex antenna impedance, except that when the resistive

component is very small compared with the reactive component, as it is under conditions near those of free space, the resistive component is poorly determined. The procedure that has been adopted is to construct a "model ionosphere" which fits the available data and to calculate the resistive component from the model. Thus we must have an appropriate theory which describes at least the resistive component of the antenna impedance as a function of electron density, over the appropriate range of parameters. The theory which has been incorporated into the OGO-IV data processing procedures is that published by Weil and Walsh (1964). This theory computes the resistive component only, and holds with adequate accuracy for the region of E-mode focussing.

We have been interested in an improved theory of antenna impedance in a plasma in order to check the adequacy of the Weil and Walsh (1964) theory in the E-mode focussing region, to provide a better means of establishing a model ionosphere, and for the intrinsic interest of the problem. The development of the theory by Weil (1970), and Lafon and Weil (1970) represents perhaps the most complete to date. Calculations based upon this theory and work by other authors (for example, Balmain, 1964) have been compared with the experiment data to a very limited extent.

III. THE EXPERIMENT AND THE SPACECRAFT

OGO-IV, the fourth spacecraft of the Orbiting Geophysical Observatory series, was launched in July, 1967 and remained in full operation until January, 1969. It was the second of the polar orbiting OGO's, and the first of the series to stabilize properly. It carried eighteen experiments, measuring various parameters of the near-earth environment, such as the energies and densities of various particles, and the strength and direction of various components of the electric and magnetic fields. The spacecraft and many of the experiments operated well for a period greatly in excess of the design life of one year.

The University of Michigan radio astronomy experiment, designated experiment 01, operated essentially full time for the entire life of the spacecraft, measuring the electromagnetic flux at frequencies of 2.0 and 2.5 MHz, and the characteristic impedance of the antenna.

A. EXPERIMENT DESCRIPTION

A complete description of the experiment is given by Yorks and Cohen (1969), and only a summary is given here.

A block diagram of the instrument is shown in figure 5. It consists of two radiometer channels, operating at 2.0 and 2.5 MHz, respectively, and an antenna impedance measuring circuit operating at 2.5 MHz. The experiment package is mounted at the far end of one of the solar panels of the OGO-IV spacecraft, with a 60 ft (19.3 m) monopole antenna mounted directly on the experiment package, and extending outward from the spacecraft.

The experiment operates countinuously, and has only one operating mode and one calibrate mode which is controlled by ground command. It produces four data outputs, each of which is sampled by the spacecraft telemetry system once during each main commutator frame, which is normally every 1/4 second.

One of the principal design objectives of the experiment was to measure the impedance of the antenna at the center frequency of the 2.5 MHz radiometer channel without interfering with the simultaneous operation of the radiometer. The measurement of impedance requires that a test signal be injected into the antenna, and such a test signal would normally interfere with the radiometer. The approach was to operate the 2.5 MHz radiometer as a zero intermediate-frequency superheterodyne circuit, with a narrow-band rejection filter centered at 2.5 MHz.

A small, constant-current signal is injected into the antenna, of such amplitude that the induced voltage never exceeds about 1 mv. The advantages of the small signal are two-fold: (1) It is easy to reject in the 2.5 MHz radiometer, and (2) it will not disturb the surrounding ionospheric medium in any way. A signal large enough to excite any non-linear process in the medium would produce misleading results in the experiment.

The composite signal in the antenna, consisting of the voltages induced by the test signal and by the ambient electromagnetic fields, is amplified by the broad-band pre-amplifier, and then distributed to the antenna impedance channel and to the two radiometer channels.

The impedance channel consists of a narrow-band pass filter centered at 2.5 MHz, followed by amplifiers driving two synchronous detectors, one measuring the in-phase component (cosine channel, corresponding roughly to the resistive component of the antenna impedance), and the other measuring the quadrature component (sine channel, corresponding roughly with the reactive component of antenna impedance).

The 2.5 MHz radiometer channel consists of a narrow-band rejection filter centered at 2.5 MHz to reject the antenna impedance test signal, followed by a mixer to inject the 2.5 MHz local oscillator signal, which is derived from the same oscillator as the impedance test signal. This operation of filtering out the 2.5 MHz signal and re-injecting it is necessary to maintain a constant amplitude local oscillator signal at the mixer. The amplitude of the test signal which is present at the antenna terminal obviously varies with the antenna impedance. The 2.5 MHz mixer is followed by a zero-frequency IF (or "audio") amplifier with automatic gain control, to give it an essentially logarithmic characteristic, and a detector. The effective bandwidth of the radiometer is 60 KHz.

The 2.0 MHz radiometer channel consists of a band-pass filter centered at 2.0 MHz which determines the frequency response of the channel, followed by an amplifier with automatic gain control, to give it an essentially logarthmic characteristic, and a detector. The effective bandwidth of the radiometer is 40 KHz.

The in-flight calibration system consists of a capacitor which is switched across the pre-amplifier input in place of the antenna in response to a ground command. To the antenna

impedance measuring channel, this capacitor represents a known impedance and constitutes a single calibration point to confirm the proper operation of the circuit. To the radiometers, this capacitor represents a source of essentially zero emission, for checking the zero point. There is no in-flight check of the radiometer gain characteristics.

B. HISTORY OF THE SPACECRAFT AND EXPERIMENT

1. Summary

OGO-IV was launched on July 28, 1967, and operated in the stabilized mode until January 23, 1969, when it was necessary to revert to a spin mode. It was operated in this mode until October 23, 1969, when, due to continued degradation of components, it was turned off. Thus the spacecraft, and most of the experiments, achieved almost eighteen months of essentially normal operation, followed by another nine months of reduced operation. It had exceeded the design objective of one year of operation by a comfortable margin.

The radio astronomy experiment, designated 01, operated essentially continuously for the entire period of stabilized operation, and for a large portion of the spin mode period, with no evidence of failures or significant degradation. Continuous data for the entire period are not available, however, because of telemetry limitations.

2. Launch

The OGO-IV launch took place from Space Launch Complex 2 of the Western Test Range, at 1421.5 UT, on July 28, 1967. The launch vehicle was a thrust-augmented Thor/Agena D. The

intended orbit, nearly circular and nearly polar, was achieved within the expected accuracy. The spacecraft was designated 1967-73A (OGO-IV). The sun and earth sensors locked on to their targets, and stabilization was achieved within a few revolutions. After confirmation of the proper operation of the spacecraft, the various booms and appendages were deployed by ground command, the radio astronomy antenna being deployed on Revolution 31.

3. Orbit

The orbit of OGO-IV is relatively low, slightly eccentric, and nearly polar, similar to the orbits of OGO's II and VI. These, the polar-orbiting OGO's, have the mission of exploring the near-earth environment and the upper ionosphere, in contrast with the eccentric OGO's (I, III, and V), which range almost halfway to the moon, exploring the magnetosphere and the cis-lunar environment. The approximate orbital elements shortly after launch are given in Table 1. Except for a rapid precession of the plane of the orbit and the position of perigee, these elements were essentially unchanged in January 1969.

The orbit has proven quite adequate for the radio astronomy experiment. On practically every revolution, the spacecraft dips into the ionosphere, passing through the critical focussing region once on the way down, and once on the way back up. Generally, these passages are well separated.

4. Attitude Oscillations

In revolution 42, about eighteen hours after the 60 foot radio astronomy antenna was erected, small oscillations were noticed in the pitch angle of the spacecraft. These oscillations increased in amplitude until, by Rev 57, the gas jets began firing to stabilize the spacecraft. It became apparent that if the spacecraft continued to operate

in this manner, the gas supply would be rapidly depleted, so the operation of the jets was inhibited by ground command while the problem was studied. A mode of operation was evolved whereby the gas jets were normally inhibited, allowing the oscillations to build up, controlled only by the reaction wheels. Then, at a convenient time when the spacecraft was in contact with a ground station, appropriate commands were sent to allow the jets to fire and to "unload" the reaction wheels. This strategy was so successful that as late as January, 1969, there was sufficient gas supply to justify a prediction of another full year of stabilized operation, if the rest of the spacecraft systems continued to function. Unforturnately, they did not, though the spacecraft exceeded its design life by a comfortable margin.

The oscillations in pitch angle have been attributed to a thermally excited motion of the 60 ft radio astronomy antenna, largely on the basis of the fact that no other appendage on the spacecraft appears to have a natural period of the proper duration (approximately 34 sec), and that the oscillations disappear during eclipse, when solar energy would not be available to excite the antenna.

5. Turn-Off

The principal events which led to the "death" of the spacecraft were the failure of the second tape recorder in January, 1969, and the failure of a power supply converter in September, 1969. The loss of the tape recorder meant an end to stabilized operation, since the semi-manual stabilization procedure which had been used since shortly after launch depended upon the availability of recorded data. It also meant that further data from the radio astronomy experiment was of very limited value. Proper interpretation of these data depend upon the spacecraft being stabilized, so that the direction of the antenna is essentially constant, and upon having continuous data extending for periods of at least 30 minutes.

After the failure of the tape recorder, the spacecraft was commanded into the spin mode to conserve the remaining gas, so that it could be restored to stabilized operation for a short period at some future date.

The failure of power supply converter No. 2 on September 13, 1969, crippled the spacecraft control system severely, and on October 23, 1969, the spacecraft was officially turned off, and no more operations were contemplated.

IV. DATA REDUCTION

It was recognized at the outset that using the ionospheric focussing phenomenon to map the celestial sphere posed a major task in data reduction. The problem has three characteristics, any one of which could make it a large task. The quantity of data to be processed is large, lengthy expressions must be evaluated, and close interplay is required between the computations and the judgement of a scientist. The first two requirements indicated that the calculations must be done by computer. The third indicated that the computer must have an on-line graphic display capability.

The facility available at the time the experiment was proposed included the tape-to-film converter (TFC), capable of off-line graphic output on 35 mm film (McCreery and Potter 1969), and the University IBM 7090 computer, which was about to be phased out in favor of a 360/67. The 360 system was planned to have graphic display capability, but not in time to support the experiment. The only workable alternative seemed to be to install a computing system which included a medium scale computer, magnetic tape, and on-line CRT display. The TFC capability would also be required.

Approval to acquire the computer was sought, and design begun on a CRT display unit that could be adapted to either on-line or off-line use. The SDS 930 computer was selected, and by early 1967 enough portions of the system were operational that we could begin partial processing of data from OGO-II.

Programs to carry out the calculations were begun, but it was necessary to move slowly, because details of the procedure did not become clear until some data were processed.

A. GENERAL PLAN

The data reduction plan for OGO-IV is built around the primary objective of the experiment, which is the generation of a map showing the distribution of cosmic radio noise at a frequency of 2.5 MHz over the celestial sphere. Data reduction procedures for the secondary objectives utilize the primary procedure as much as possible.

For convenience, the procedure is divided into five parts:

Part 1 Plot the experiment output on film. Evaluate the data for each orbit, and identify "selected intervals" of time when focussing may have occurred.

Part 2 Reduce the radiometer data for the selected intervals from telemetry units to mean square noise voltage at the radiometer input, and the antenna impedance data to resistance and reactance.

Part 3 Fit a model ionosphere to the observed data for a selected interval, and calculate better values of the antenna resistance. Correct for the impedance match between the antenna and radiometer, and for the radiometer internal noise. Separate the ordinary and extra-ordinary modes. Determine the time when focussing occurred in the extra-ordinary mode, and the value of the cosmic noise temperature observed at that time.

Part 4 Determine the effective region of the celestial sphere from which the antenna is receiving radiation (effective beam).

Part 5 Combine many such measurements into a map of the effective cosmic noise temperature over the celestial sphere.

B. PART 1 PROCEDURE

In Part 1, the unreduced experiment data is plotted as a function of time, on 35 mm film. The reduction procedure requires at least 30 minutes of uninterrupted data, and preferably an entire orbit. Therefore the only data which is plotted is that from "playback tapes": those for which data is accumulated in the spacecraft tape recorders for an extended period of time, and then telemetered to the ground. "Real time" tapes, which contain only short intervals of data, are not used for this purpose.

The film format for the Part 1 output is illustrated in Figure 6. Wherever possible, an entire orbit is plotted, preceded by a title frame which includes the reference data necessary to interpret the plots; principally the date and time. The four principal experiment outputs are plotted as functions time: 2.0 MHz radiometer, 2.5 MHz radiometer, and the sine and cosine channels of the antenna impedance meter. No housekeeping or spacecraft status data is plotted. The data are plotted in units of voltage at the experiment output terminals, which has a range from 0 to 5.1 volts. The plots are divided into two portions, an upper portion with a scale of 0 to 5.1 volts, where the 2.0 MHz radiometer and the sine channel are plotted and a lower portion with a scale of 0 to 5.1 volts, where the 2.5 MHz radiometer and the cosine channel are plotted. (The sine

channel can be more or less identified with antenna reactance, while the cosine channel can be identified with antenna resistance). Horizontal grid lines are drawn at 0, 1, 2, 3, 4, and 5.1 volts.

The time scale is marked by a vertical grid line every ten minutes, with a break in the scale at 50 minutes where the film was advanced between frames. The two frames thus represent a period of 100 minutes, slightly longer than the OGO-IV orbit period. No numbers appear on the time scale. It is necessary to refer to the start time given in the title frame, and count forward to determine the actual Universal Time.

A title frame is inserted at the beginning of every data file, and every 98 minutes thereafter. It consists of:

1. The spacecraft identity: "D" for OGO-IV, "C" for OGO-II.
2. A number identifying the telemetry ground station which received the data.
3. The UM/RAO number assigned to the experiment data tape (not the TFC tape) from which the data came.
4. The file number on the experiment tape.
5. The record number on the experiment tape of the first record plotted.
6. The month, day, and year of the start of the plotted data.
7. The Universal Time (hours and minutes) of the start of the plotted data.
8. The approximate number of minutes from the beginning of the plot to the perigee time for this orbit.

Note that the start time for a plot is not necessarily the start time for an orbit, as normally defined in the orbit data (the ascending mode), but rather depends upon the start time of a data fill on the experiment tape.

The Part 1 films are visually inspected with the following objectives:

1. To pick "selected intervals" for the Part 2 and subsequent processing.
2. To monitor the performance of the experiment and the spacecraft.
3. To monitor the characteristics of the ionosphere, to the extent that its characteristics affect the success of the experiment.
4. To search for effects which may bear upon the secondary objectives of the experiment.
5. To search for effects which may represent discoveries of phenomena which were not anticipated.

The selected intervals which are carried through the Part 2 and subsequent steps are normally ten minutes in duration, and are centered upon the time when the spacecraft passes through the level in the ionosphere where focussing should occur. This level is recognized from the behavior of the experiment data. Figures A-1 and A-3, Appendix A, show the characteristic events of typical "passes", during which the spacecraft moved downward through the focussing level. The most conspicuous feature is the rise of the sine channel, followed by a sharp drop, and then usually by a modest increase. The cosine channel rises, reaching a maximum at about the time the sine channel drops sharply. The 2.5 MHz radiometer shows a minumum just before the sine channel drop, while the 2.0 MHz radiometer shows a minimum somewhat earlier, and usually less clean cut.

A pass upward through the focussing level shows the same events, in reverse order.

Only "clean" passes are selected for further processing. If the events of a pass are grossly distorted, it is probably because the ionosphere in this region is disturbed, and does not approach the assumption of plane-parallel stratification which is required in Part 3.

C. PART 2 PROCEDURE

Part 2 is a preparatory step for Part 3, performed on the computer. The Part 2 program accepts specifications for selected intervals on punched cards, searches the experiment data tapes for these intervals, converts the data from telemetry units to scientific units by applying a correction for the instrument characteristics, and writes the data on a magnetic tape, ready for input to Part 3.

Data from both radiometer channels is converted from radiometer output voltage to mean square noise voltage at the radiometer inputs. The conversion is performed by interpolating in a table of radiometer output vs input. This table is based upon the preflight calibration of the radiometers.

Data from the antenna impedance channels is converted from experiment output voltage to resistance and reactance, expressed in ohms, using a pair of equations which describe the characteristics of the experiment package. Certain constants in these equations are derived from preflight calibration.

The Part 2 procedure results in a considerable concentration of the data. Data from several experiment data tapes are concentrated on a single output tape.

D. PART 3 PROCEDURE

Part 3 is the key step, which determines the antenna temperature in the focussing region, and the ionosphere parameters that are necessary to Parts 4 and 5. The input data for a Part 3 run is a single selected interval; a ten-minute period of data including a single passage of the S/C through the focussing layers of the ionosphere.

The antenna temperature, of course, is to be identified with the brightness temperature of the portion of the celestial sphere that is within the "beam". To determine the antenna temperature, it is necessary to know not only the radiometer input voltage, but also the antenna radiation resistance, and the power transfer factor between the antenna and the radiometer, which is a function of the complex impedance of the antenna. The experiment itself includes instrumentation for measuring the resistive and reactive components of the impedance, but over a portion of the focussing region the resistance is so small compared with the reactance that it cannot be measured with sufficient accuracy. The general strategy in Part 3 is to find a "model ionosphere" which fits the observed data, and then to compute the radiation resistance over the focussing region using this model.

Part 3 makes repeated use of a computer-aided curve fitting procedure which uses the SDS 930 computer and on-line display facility described in Appendix C. In this

procedure, the computer generates a synthetic curve, using appropriate equations, which it presents to the scientist superposed upon the observed points. The scientist then adjusts appropriate parameters in the equation until the synthetic curve is brought into agreement with the observed curve.

Steps of the Part 3 Procedure:

The first step in the Part 3 procedure is to search the attitude orbit tapes for the spacecraft position data and magnetic field data for the selected interval. These data are read from tape and stored in the computer. The experiment data for the selected interval are then read from the tape of processed data which was prepared by the Part 2 programs.

The computer then presents on the CRT display a pair of curves representing the measured antenna resistance and reactance, for evaluation by the scientist. Next, it presents the data from the two radiometer channels, one at a time. For each channel, the scientist attempts to identify the "E-mode cutoff" point -- the level in the ionosphere below which the extra-ordinary mode cannot propagate. Knowing the magnetic field, it is easy to compute the electron density at this point. Thus each radiometer channel yields a value of the ambient electron density at a point along the S/C path. We fit a simple exponential function to these points, which serves as an initial model ionosphere.

The model ionosphere is improved by successive approximations. Using the model ionosphere and the magnetic field, the computer determines the theoretical radiation resistance, the power transfer factor from the antenna to the radiometer, and the general form of the variation with time of the radiometer signal, for each channel. This "synthetic" radiometer

signal is presented on the CRT, together with the observed radiometer signal. The scientist compares the two, and, if the fit is not satisfactory, he makes adjustments to the model ionosphere, and directs the computer to generate a new set of synthetic radiometer signals.

The next step is the correction for the noise which is generated internally to the radiometer. This contribution is computed, using parameters which were determined from the pre-flight calibration of the instrument, and subtracted from the observed signal. This correction is always small.

The next step is to separate the contributions of the two modes of propagation in the bi-refringent medium. We wish to retain only the contribution of the extra-ordinary mode (or E-mode). We assume that, in the region of E-mode focussing, the ordinary mode (0-mode) still "sees" an entire hemisphere, and hence is not changing with time. We evaluate the 0-mode contribution by computing a synthetic radiometer signal for 0-mode only, using the computer 0-mode component of the radiation resistance, and using an assumed value for the effective antenna temperature in the 0-mode. We then compare the synthetic 0-mode curve with the observed radiometer output curve, and adjust the 0-mode brightness temperature until a fit is obtained over that portion of the observed curve that lies below the E-mode cutoff, where only 0-mode propagation is received. This synthetic curve is assumed to adequately represent the 0-mode contribution in the region above the E-mode cutoff also, and is subtracted from the total observed signal to obtain the observed E-mode signal.

The last step in the Part 3 procedure is to record the E-mode brightness temperature at selected points in time as the spacecraft passed through the focussing region. A synthetic E-mode curve is generated, using the E-mode antenna resistance which was computed from the model ionosphere, and an assumed brightness temperature. The temperature is adjusted until the synthetic E-mode curve fits the observed curve over some interval of time. Then both the E-mode antenna temperature and the time are recorded. Sufficient points are recorded to adequately define any variations in E-mode temperature that occur in the focussing region. These points are passed on to Part 4 of the processing procedure, to be used in constructing a map of the cosmic background temperature.

E. PART 4 AND 5 PROCEDURE

Parts 4 and 5 of the procedure are not completely defined, because no data has been processed through these steps. The objective of Part 4 is to define the angular size and position of the effective antenna beam upon the celestial sphere, and the objective of Part 5 is to combine many such observations into a map of the distribution of cosmic noise temperature at 2.5 MHz.

In preparation for Part 4, methods have been developed for computing the effective beam pattern, given the model ionosphere and the magnetic field. (See Section II-B, above). The Part 4 procedure, then, consists of carrying out this computation for each of the points recorded in Part 3. Detailed beam contours can be computed, but it will probably suffice to compute the celestial coordinates of the effective beam center, and some measure of the effective beam diameter. These parameters, together with the effective antenna temperature, form the input data to Part 5.

Part 5 is a manual process, where each antenna temperature is recorded on a chart at the proper location, with some notation of the effective beam diameter. As data accumulate on the chart, it should be possible to check for internal consistency among the measurements which cover the same area, and to construct the contours of constant brightness temperature which are the objective of the experiment.

F. IONOSPHERIC DATA AND ANTENNA IMPEDANCE

A secondary objective of the experiment, and a necessary bi-product of the ionosphere focussing experiment, is the study of the ionosphere, and the behavior of antennas in it.

The behavior of an antenna in a magneto-plasma, such as the earth's ionosphere, is very complex. There exists no theory which is complete, general, and exact. If such a theory did exist, it would, in all likelihood, be too cumbersome for practical computation. Available theories either neglect the effect of certain physical processes, such as collisions, make simplifying assumptions about the antenna geometry, or make simplifying assumptions about the current distribution in the antenna.

Various laboratory experiments have been performed which, in general way, confirm the validity of some of these approximations under certain conditions. Unfortunately, it is impossible to duplicate in the laboratory the conditions encountered in the earth's ionosphere. Thus the experimental data are not applicable to the ionospheric focussing experiment, and the theory is inadequate to extrapolate from laboratory conditions to ionosphere conditions.

The antenna impedance data from the OGO-IV experiment constitutes a large body of experimental data, against which the theory can be tested. The six hundred selected intervals which were extracted and reduced for the focussing experiment also represent useful periods for which to study the antenna impedance, since they include the region where the antenna impedance is most sensitive to the ionospheric parameters. The applicability of any theory to ionospheric conditions, then, can be tested by comparing it with the observed data. The theory should reproduce, at least in a general way, the form of the variation of antenna resistance and reactance which is observed as the spacecraft descends through the critical levels in the ionosphere.

G. RESULTS

1. Forms of Data

OGO-IV data now exists in the following forms:

(1) The experiment data tapes, received from GSFC.

(2) Unreduced data plotted on 35 mm film.

(3) A catalog of over 600 selected intervals.

(4) Magnetic tapes containing reduced data for the selected intervals.

(5) Reduced data for 36 very good selected intervals, plotted in high-resolution form.

(6) Collections of prints made from portions of the unreduced films, selected for various special purposes.

2. Experiment Data Tapes

Approximately 700 experiment data tapes were received from GSFC prior to October 1969. These tapes contain data from the launch date (July 30, 1967) through May, 1969. The attitude/orbit tapes give reasonably complete coverage through revolution 4300, on May 15, 1968. Data for the latter part of 1968, when the spacecraft and the experiment

were still operating well, is still being processed by GSFC.

All 1 kilobit playback data have been processed through the Part procedure, which generates a plot of the experiment data on 35 mm film.

The data tapes were retained, because the subsequent steps in the processing refer back to the tapes.

3. Film Plots

All 1 kilobit playback data has been plotted on 35 mm film, in unreduced form. Figure 6 is an example of the format. Three frames of film are allotted to each spacecraft orbit, the first frame containing the identifying parameters, the last two the plotted data. The time scale is compressed so that an entire orbit (98 min) occupies only 1.5 in of film. The four experiment output voltages are plotted against time, with no processing or corrections.

4. Catalog of Selected Intervals

A catalog of over six hundred selected intervals has been prepared. A selected interval is a ten minute block of data containing a passage of the spacecraft through the critical levels of the ionosphere, where focussing should have occurred. The catalog was prepared by inspecting the film plots, and hence includes only passages where the data is good enough, and the ionosphere is uniform enough, that the phenomena which accompany such a passage are recognizable. For each selected interval, the catalog lists the date and time, the necessary information to retrieve the original data from the experiment data tapes, and some information on the passage itself, i.e., whether it is upward or downward, and a crude evaluation of the quality of the data: good, fair, or poor.

5. Processed Data Tapes

Data for each of the selected intervals have been reduced to scientific units, and recorded on magnetic tape. Appendix B describes the format of these tapes. Eleven tapes are required.

The tape includes identity and reference information for each selected interval, and reduced experiment data for every telemetry sample during the selected interval. The radiometer data are reduced to mean square noise voltage at the radiometer terminals, and the antenna impedance data are reduced to antenna resistance and reactance, in ohms. These reductions are performed using values of the instrument parameters which are appropriate to the environmental conditions which exist in the spacecraft most of the time. For those periods of time when an abnormal condition exists in the spacecraft, a more accurate reduction could be obtained by using different values of the experiment parameters. This has not been done in producing these tapes.

These processed data tapes are intended primarily to serve as input for Part 3 of the processing procedure. However, they contain most of the information which would be useful for analyzing the behavior of the antenna impedance in the general vicinity of the plasma frequency.

6. High Resolution Plots of Very Good Intervals

Thirty-six of the selected intervals were classified as "very good", and were plotted in high resolution form. These plots illustrate the sequence of events observed as the spacecraft passes through the critical levels in the ionosphere, in both the radiometers and the antenna impedance meter.

7. Special Collection of Prints

Several sets of prints have been made from portions of the unreduced film plots, to answer specific questions. For instance, sets of prints have been made which show OGO-IV data at times when low frequency solar bursts were observed by other space experiments. A set of prints has been made of selected intervals when the focus point should be in the region of the galactic pole, and another set where the focus point should be in the region of the galactic plane. Sets of prints have been made to illustrate various kinds of ionospheric anomalies, such as the regions of high electron density which show quite conspicously in the film plots.

V. CONCLUSIONS

A. SUMMARY

The primary purpose of the OGO-IV radio astronomy experiment was the mapping of the brightness temperature of the celestial sphere at a frequency of 2.5 MHz using the ionospheric focussing effect. Because of the high level of radio-frequency interference generated in the spacecraft, it seems unlikely that mapping information can be extracted from the data. In any event, the presence of the interference would make the extraction of mapping information more difficult than anticipated. The data have been extensively studied, with negative results to data.

The antenna impedance channels of the instrument are not affected by the interference, and present a wealth of data on the ionosphere and the behavior of the antenna impedance. Some phenomena, such as the "third reactance flip", discussed in section C, below, seem to be previously unreported. Their significance should be investigated. The OGO-IV data include several hundred instances where the spacecraft passed upward or downward through the critical levels of the ionosphere in regions that appear to be free of local inhomogeneities, so that the ambient electron denstiy was a smooth, monotonic function of time. Thus the functional dependence of the antenna impedance on electron density is well exhibited. Any theory of antenna impedance in a plasma must be consistent with these observations.

B. MAPPING THE COSMIC BACKGROUND

Because of the high level of radio-frequency interference generated in the spacecraft, we have been unable to extract the necessary information to produce the intended map of the brightness temperature of the cosmic background at 2.5 MHz. It is possible, though not likely, that a more complex and detailed procedure of analysis could be evolved, which would make possible the extraction of some mapping information.

There is no reason to question the validity of the original experiment concept, nor the design of the experiment itself. The interference generated in the spacecraft seems to be the only obstacle to success.

1. Level of Interference

The level of interference experienced on OGO-IV is considerably less than that experienced by the identical experiment on OGO-II. Thus the interference suppression measures taken as the result of the OGO-II experience were at least partially successful. The OGO-IV radiometers are not saturated under normal conditions, as were these on OGO-II, though they are always operating in the upper portion of their range. The radiometers are designed to operate over a dynamic range greater than three orders of magnitude.

The interference level is greater than the expected cosmic background signal. We may compute the expected signal from the cosmic background by the equation:

$$V^2 = 4\ kB\ T_A R_A \quad \frac{R_L^2}{(R_A + R_L)^2 + X_A^2} \qquad (V\text{-}1)$$

where V^2 = Mean square noise voltage at the radiometer input

k = Boltzman's constant = 1.38×10^{-23} joules/deg

B = The radiometer bandwidth = 60 kHz,

T_A = The effective noise temperature of the antenna

R_A = The radiation resistance of the antenna

R_L = The radiometer input impedance = 2500Ω

X_A = The effective antenna reactance

The expected brightness temperature for the cosmic background at 2.5 MHz is about 1.7×10^7 K. R_A and X_A vary widely, as the spacecraft moves down into the ionosphere. If we substitute value of R_A and X_A appropriate to free space, we find that the signal expected from the cosmic background is more than two orders of magnitude below the observed signal. If, however, we substitute values of R_A and X_A that are measured in the focussing region, we find that the expected cosmic background is about 1/10 of the observed signal. Thus it may be possible to extract the cosmic contribution from the total signal, but only if the contribution due to spacecraft interference can be evaluated with an accuracy which is significantly better than 10%.

Most of the interference appears to be radiated to the radio astronomy antenna from other parts of the spacecraft, since little interference was observed before the antenna was erected. Obviously, the properties of the ambient ionosphere greatly affect the level of interference reaching the antenna, since the level varies by as much as two orders of magnitude as the spacecraft passes through the critical

levels in the ionosphere. To account for this variation would be difficult, since it entails determining the effect of the ionosphere on the radiation resistance of the unidentified emitting surfaces of the spacecraft, and determining the near-field propagation characteristics of the ionospheric plasma.

2. A Possible Procedure for Interpretation

It is possible at this point to list some of the properties required of a successful procedure to deduce a map of cosmic brightness temperature at 2.5 MHz from the existing OGO-IV data, in the face of the high interference levels.

(1) Deduce a model ionosphere primarily from the measured antenna impedance data. The original plan was to deduce the model ionosphere from the E-mode breakout points for 2.0 and 2.5 MHz, respectively, as observed in the radiometer. The breakout points are obscured by interference, so it is necessary to base the model on the impedance data, which are not bothered by interference.

(2) Evaluate the interference level, and compute the contribution of interference as a function of time, as the spacecraft passes through the focussing level. This is the difficult step mentioned above, and may not be possible.

(3) Subtract the interference contribution, leaving the cosmic contribution. A test of the validity of the operation may be made at this point by searching for the E- and 0-mode dropouts. If they appear at points consistent with the antenna impedance data, then the procedure may be assummed to have been carried out in a valid manner, and significant cosmic radiation has been detected.

It should then be possible to extract the mapping information using the original procedure.

C. INVESTIGATION OF THE IONOSPHERE

1. General

The study of the ionosphere was not, of course, the primary objective of the OGO-IV experiment. Nevertheless, the experiment has yielded a large quantity of data about the top-side ionosphere. Very little reduction and interpretation has been performed on this aspect of the data, however.

The OGO-IV experiment provides two independent means of probing the ambient ionosphere: a direct probe by the antenna impedance measurement, and an indirect probe by the radiometer channels. Both of these are sensitive indicators only when the electron density is such that the plasma frequency is in the general vicinity of 2.0 to 2.5 MHz, but are extremely sensitive within that range. There is some indication that the so called "second and third reactance flips" which are observed in the data may be interpreted so as to yield a measure of electron density in a range considerably above the plasma frequency, but these phenomena are not sufficiently well understood at present.

When an antenna is immersed in an ionized medium, such as the earth's ionosphere, its characteristic impedance may be drastically altered from the free space value, because the index of refraction of the medium may be drastically altered. (Section IV, D, below, gives a brief account of the behavior of the antenna impedance, and Section II, B is a short description of the behavior of the index of refraction). Even though the theory of the characteristic

impedance of antennas immersed in plasmas is very complex and is still an active area of research (see, for example, Weil, 1970, and Lafon and Weil, 1970), it is still possible under favorable conditions, to find useful solutions to the reverse problem of determining the electron density, given the antenna impedance. Thus antenna impedance data measured on OGO-II have been used to map the wake of the spacecraft by using the fact that the antenna sometimes passes through the wake as the spacecraft spins (Yorks, Weil, and Potter, 1968; and Weil and Yorks, 1969).

The impedance data from the OGO-IV experiment could be used to derive fairly reliable figures for the ambient electron density along segments of the spacecraft orbit which typically extend over some 10 to 20° of geographic latitude. Over 600 such intervals have been identified in the data during which both the antenna impedance data and the radiometer data appear usable, and there is no evidence of small scale irregularities in the ionosphere. There are many other cases where small scale irregularities are present, which may be of equal interest in ionosphere analysis.

The electron density which one derives from the measured impedance of a 60 ft antenna would be weighted mean over a volume at least as long as the antenna, and at least a few meters in diameter. Thus the measurement is not likely to be affected by local disturbances of the medium by the passage of the spacecraft when the antenna is not in the spacecraft wake. Since the OGO-IV spacecraft was properly stabilized during its entire useful life, the orientation of the antenna is known at all times, so there need be no contamination from this source. Thus the antenna impedance method offers some advantages over instruments such as the Langmuir probe.

The second method for determining the ambient electron density from the OGO-IV experiment is based upon the cutoff points for the E-mode and 0-mode propagation in the ionosphere. This method has a straight-forward theoretical basis, since it depends only upon the refractive index of the medium, and not upon the effect of the medium on the antenna. As discussed in Section II, B, electromagnetic radiation impinging from outside the ionosphere cannot penetrate below the level where the index of refraction reaches zero. The cutoff level differs for the two modes of propagation, and as the spacecraft moves down into the ionosphere, we would expect half of the radiation from outside the ionosphere to disappear at the E-mode cutoff level ($X = 1-Y$), and the other half to disappear at the 0-mode cutoff level ($X = 1$). If these cutoff points can be observed, we can establish the electron density at four points in the ionosphere (two modes at two frequencies) for each passage of the spacecraft.

In OGO-IV, the radiometer channels are subjected to a high level of internally-generated interference which makes it impossible to specifically identify the two cutoff points with precision. There is a distinct and dramatic reduction in the signal at the radiometer inputs as the spacecraft moves through the cutoff region, however, due partly to the change in antenna impedance, but probably due at least in part to the failure of the medium to propagate even internally generated radiation from the spacecraft itself to the antenna, as well as the cutoff of externally generated radiation. Comparison of the 2.5 MHz radiometer with the 2.5 MHz antenna impedance confirms this assumption. At 2.5 MHz the antenna impedance gives a much better indication of electron density than the radiometer data, but we have no antenna impedance data at 2.0 MHz. At 2.0 MHz, the radiometer data can be expected to yield estimates of the time of cutoff that are good to at least a minute, and

perhaps better.

D. ANTENNA IMPEDANCE IN A PLASMA

1. General

The OGO-IV experiment has generated many thousand measurements of the characteristic impedance of the antenna, measured under a range of conditions which is difficult to reproduce in the laboratory. These measurements should, therefore, consititute a valuable test of the theory of antenna impedance in a plasma. Direct interpretation of the data is difficult, because the experiment was not designed primarily for this purpose. The experiment has demonstrated, however, that effective measurements of the impedance of an electrically short antenna can be made in space, using simple and reliable equipment. Further, the impedance measurement can proceed simultaneously, and at the same frequency, as radiometer operations.

2. Comparison with Theory

Some comparisons have been made between the OGO-IV antenna impedance data and theory. Yorks has compared the theory due to Balmain (1964) with some OGO-IV data. He finds general agreement, but important difference in detail. Comparison has been made with the development by Weil (1970), but because of the length of the numerical calculations these comparisons have not been carried out to a useful extent.

3. The "Third Reactance Flip" Phenomenon

Many OGO-IV passages through the ionosphere exhibit a previously unreported phenomenon, which we have referred to as the "third reactance flip". In the experiment data,

the phenomenon has the appearance of a miniature replica of principal reactance flip near X = 1, only occurring at a much higher electron density. An example is shown in Figure 7 where the principal flip occurs at the left, and the third flip a little later. For many passages, the events are well displayed in reverse order at the spacecraft moves back up through the ionosphere. The phenomenon is present on all passages where the data is clean and the ionosphere is uniform, and where the spacecraft penetrates far enough into the ionosphere.

The sequence of events in the third flip is that, as electron density increases, both the resistive and reactive components of the antenna impedance increase in magnitude until the resistance reaches a maximum. At about this point, the reactance abruptly changes sign. Then both components decrease in magnitude again. On a Smith chart, the complex impedance traces a spiral, as shown in Figure 8. A "second reactance flip" occurs as the reactance changes from inductive to capacitive between the first and third flips, but the second flip occurs gradually, and at a time when the resistance is small, so this flip is not conspicuous.

We cannot at this time completely rule out the possibility that the third flip is an artifact of the experiment, due perhaps to some spurious frequency component in the antenna impedance meter. Since the radiometer shows a fluctuation at the time of the third flip, we must postulate a mechanism which produces spurious responses in the radiometer also. The closely integrated nature of the radiometer and the impedance meter opens the door to such possibilities, but

we know of no mechanism that would produce a resonance in this range of plasma parameters X and Y, regardless of the length of the appendage.

We know of no theory of antenna impedance in a plasma that is consistent with the observed third flip. It would be extremely valuable to have more precise information on the conditions where it occurs, and to have independent confirmation of its existence, particularly with an antenna of simple geometry.

4. Recommendations for Future Antenna Impedance Experiments

As a result of experience gained with OGO-IV, some recommendations can be made for any future experiments designed to measure antenna impedance in the ionosphere.

The antenna geometry should be kept simple. A dipole is probably best, but a monopole with ground plane can be used, provided a true ground plane is available. The spacecraft body used on OGO-IV is too small to constitute a true ground plane. Hence the true geometry of the antenna is so complex as to be unmanageable.

Several frequencies should be used. The design of the OGO-IV antenna impedance meter is such that it could readily be extended to switch between several frequencies, or to operate on several frequencies simultaneously. The use of several frequencies will permit exploration of a much broader range of parameters, and will provide a method of determining the parameters. A broad range of frequencies is particularly necessary to explore a broad range of the parameter $Y = f_g/f$.

The earth's magnetic field does not vary over a wide range in the ionosphere, and hence a wide range of Y can be attained only by using a wide range of the operating frequency, f. Furthermore, if several frequencies are used simultaneously, at least one frequency should be in the proper range to permit calculations of the local plasma frequency.

An eccentric orbit would extend the range of parameters.

Some provision should be made for measuring the impedance with the antenna at various angles with respect to the magnetic field. The angle could be varied by rotating the spacecraft, but a preferable scheme might be to provide three orthogonal dipoles.

REFERENCES

Alexander, J. A., et al. 1969, Astrophys. J. 157, No. 3, Pt. 2., pL163.

Balmain, K. G. 1964, IEEE Trans. Ant. and Prop. AP-12, p605.

Bridle, A. H., and Purton, C. R. 1968, Astron. J. 73, No. 8, p717.

Ellis, G. R. A. 1957, J. Geophys. Res. 62, p229.

Ellis, G. R. A. 1964, Nature 204, p 171.

Ellis, G. R. A. 1965, Mon. Notices, Royal Astron. Soc. 130, p429.

Ellis, G. R. A., and Hamilton, P. A. 1964, Nature 204, p272.

Ellis, G. R. A., and Hamilton, P. A. 1966a, Astrophys. J. 143, No. 1, p227.

Ellis, G. R. A., and Hamilton, P. A. 1966b, Astrophys. J. 146, No. 1, p78.

Ellis, G. R. A., Waterworth, M. D., and Bessel, M. S. 1962, Nature 196, p1070.

Haddock, F. T. 1962a, Proposal: "Low Frequency Cosmic Noise Survey." Submitted to GSFC, NASA, April 1962.

Haddock, F. T. 1962b, "Review of Radio Astronomy Experiment Proposed for the POGO Satellite." Submitted to GSFC, NASA, Spetember 1962.

Haddock, F. T. 1963, Proposal: "Instrumentation and Pre-Launch Activity for a Radio Astronomy Experiment for POGO." Submitted to GSFC, NASA, March, 1963.

Haddock, F. T. 1964a, Proposal: "POGO Extension Proposal." Submitted to GSFC, NASA, April, 1964.

Haddock, F. T. 1964b, Proposal: "Data Reduction and Analysis for OGO-C and -D." Submitted to GSFC, NASA, November 1964.

Haddock, F. T. 1966, "Phase 1 Final Report: Engineering Feasibility Study for a Kilometer-wave Orbiting Telescope." Submitted to NASA, October, 1966. Grant NGR 23-005-131.

Haddock, F. T. 1968a, Proposal: "The Continuation of Data Reduction and Analysis of OGO-D Data." Submitted to GSFC, NASA, April, 1968.

Haddock, F. T. 1968b, Proposal: "OGO-II Data Analysis Satellite Plasma Wake Study." Submitted to NASA Headquarters-OSSA, June, 1968.

Haddock, F. T. 1968c, Proposal: The Continuation of Data Reduction and Analysis of OGO-IV Data." Submitted to GSFC, NASA, November 1968.

Lafon, J. P., and Weil, H. 1970, Radio Science, (To be published in August 1970).

McCreery, D. R., and Potter, W. H. 1969, "The Tape-to-Film Converter" UM/RAO Report No. 69-1. January, 1969.

Potter, W. H. 1968, "Data Reduction and Analysis Report for the Radio Astronomy Experiment Aboard the OGO-II Spacecraft." UM/RAO Report No. 68-12. Submitted to GSFC, NASA, Autust 1968. Contract NAS5-3099.

Scheuer, P. A. G., and Williams, P. J. S. 1968, Ann. Rev. Astron. and Astrophys. Vol. 6, p321.

Walsh, D., and Weil, H. 1968, Radio Science 3, (new series), p9.

Weil, H. 1970, Radio Science, (to be published in April, 1970).

Weil, H., and Walsh, D. 1964, IEEE Trans. Ant. and Prop. Vol. AP-12, No. 3.

Weil, H., and Walsh, D. 1967, Radio Science, Vol. 2, (new series).

Weil, H., and Yorks, R. G. 1970, Planet. and Space Sci. (To be published).

Yorks, R. G., and Cohen, G. S. 1969, "Instrumentation for Measurement of Cosmic Noise at 2.0 and 2.5 MHz from a Polar Orbiting Geophysical Observatory." UM/RAO Report 69-15. Submitted to GSFC, NASA, Contract NAS5-3099.

Yorks, R. G., Weil, H., and Potter, W. H. 1968, "Impedance Variations of a Monopole Antenna Passing Through A Satellite's Wake." Presented to Fall URSI Meeting, Northeastern University, Boston, Mass., September, 1968.

Yorks, R. G., and Weil, H. 1970, "OGO-II Data Analysis Satellite Plasma Wake Study, Final Report." UM/RAO Report No. 70-1. Submitted to NASA, Grant NGR 23-005-068.

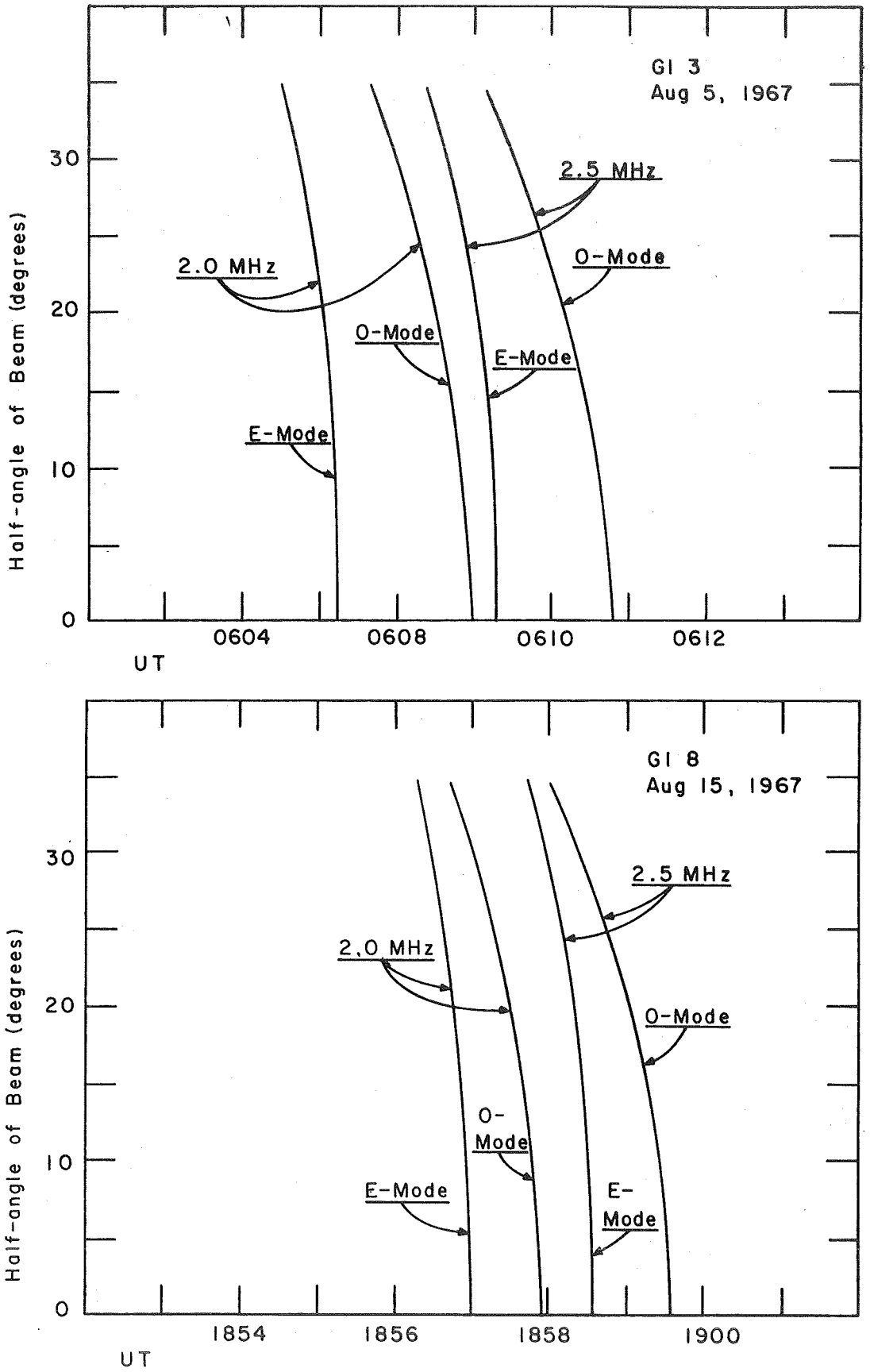

Figure 1. Half-angle of Beam as a Function of Time, for Two OGO-IV Passages.

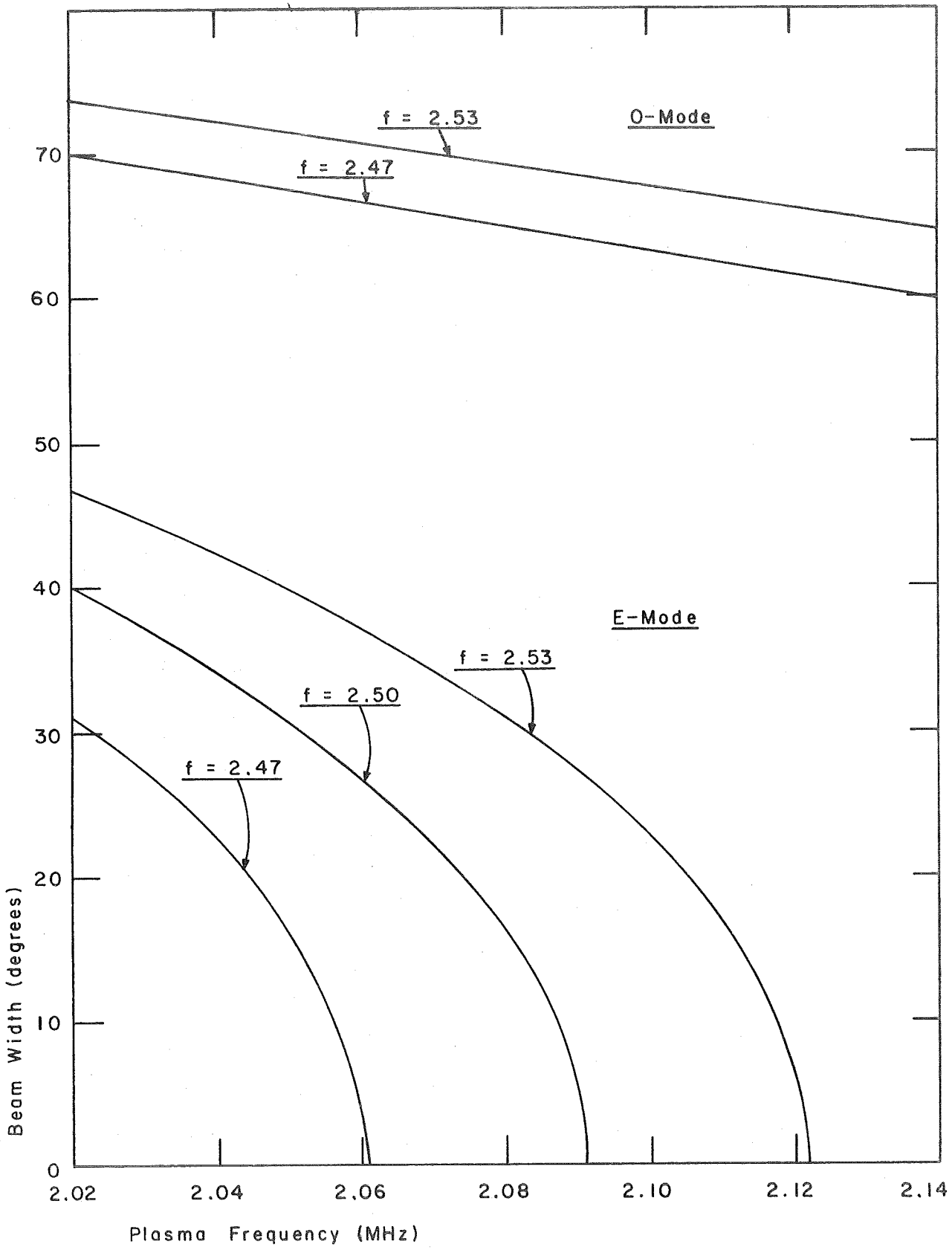

Figure 2. Bandwidth Defocussing in E-Mode, Y = 0.30.

Beam width for the center frequency and passband edges for the 2.5 MHz radiometer, as a function of plasma frequency.

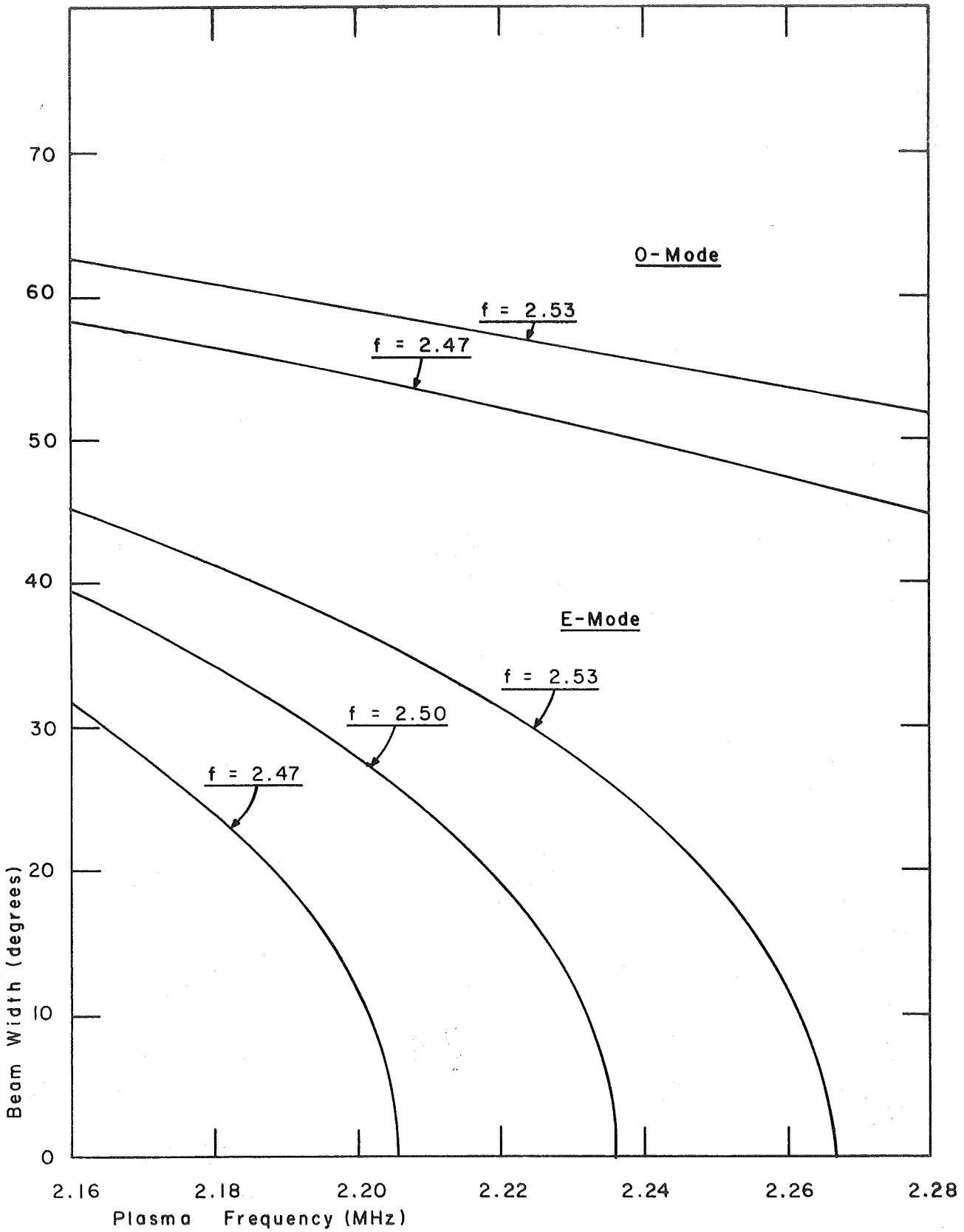

Figure 3, Bandwidth Defocussing in E-Mode, Y = 0.20.

Beam width for the center frequency and passband edges for the 2.5 MHz radiometer, as a function of plasma frequency.

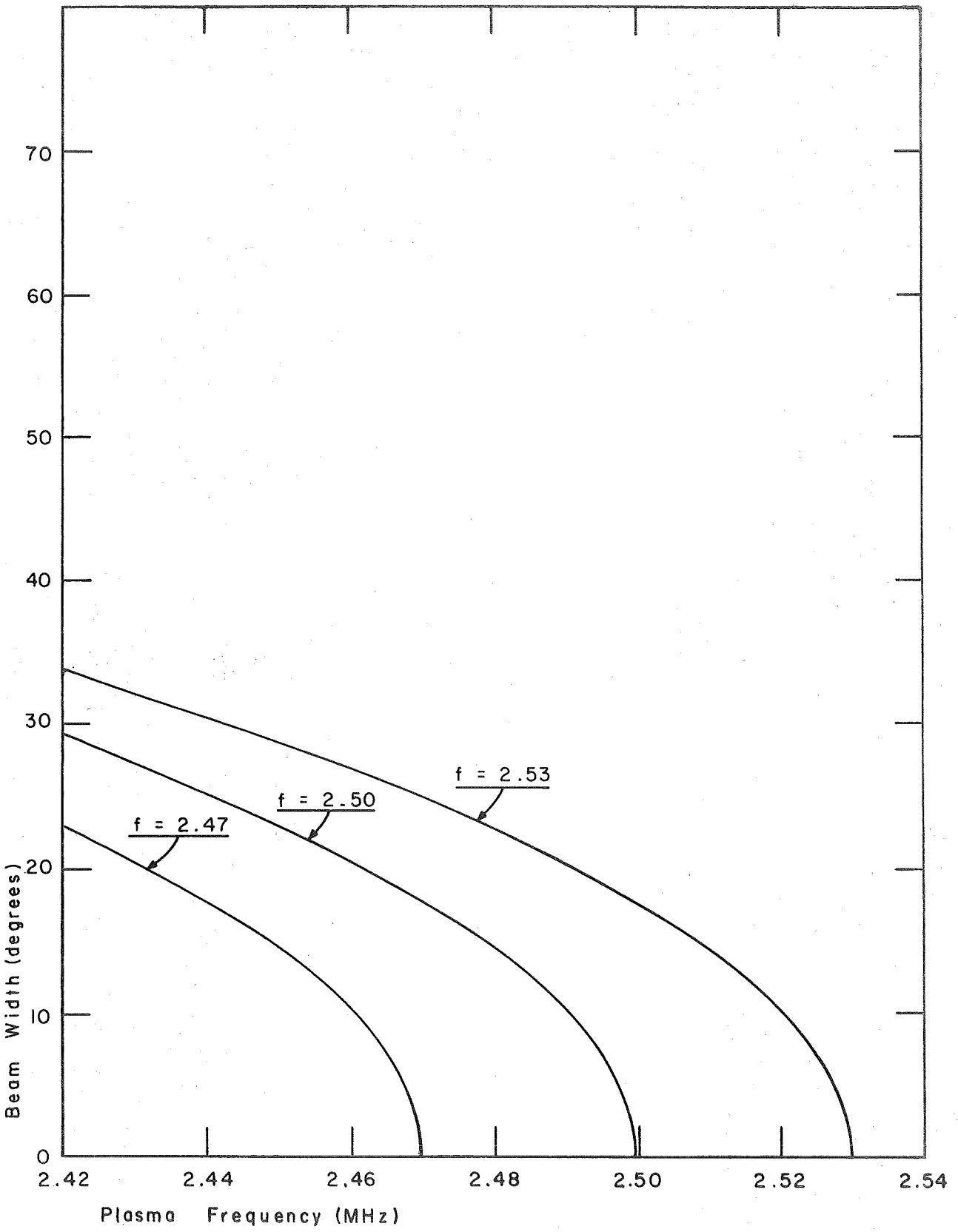

Figure 4. Bandwidth Defocussing in O-Mode.

Beam width for the center frequency and passband edges for the 2.5 MHz radiometer, as a function of plasma frequency.

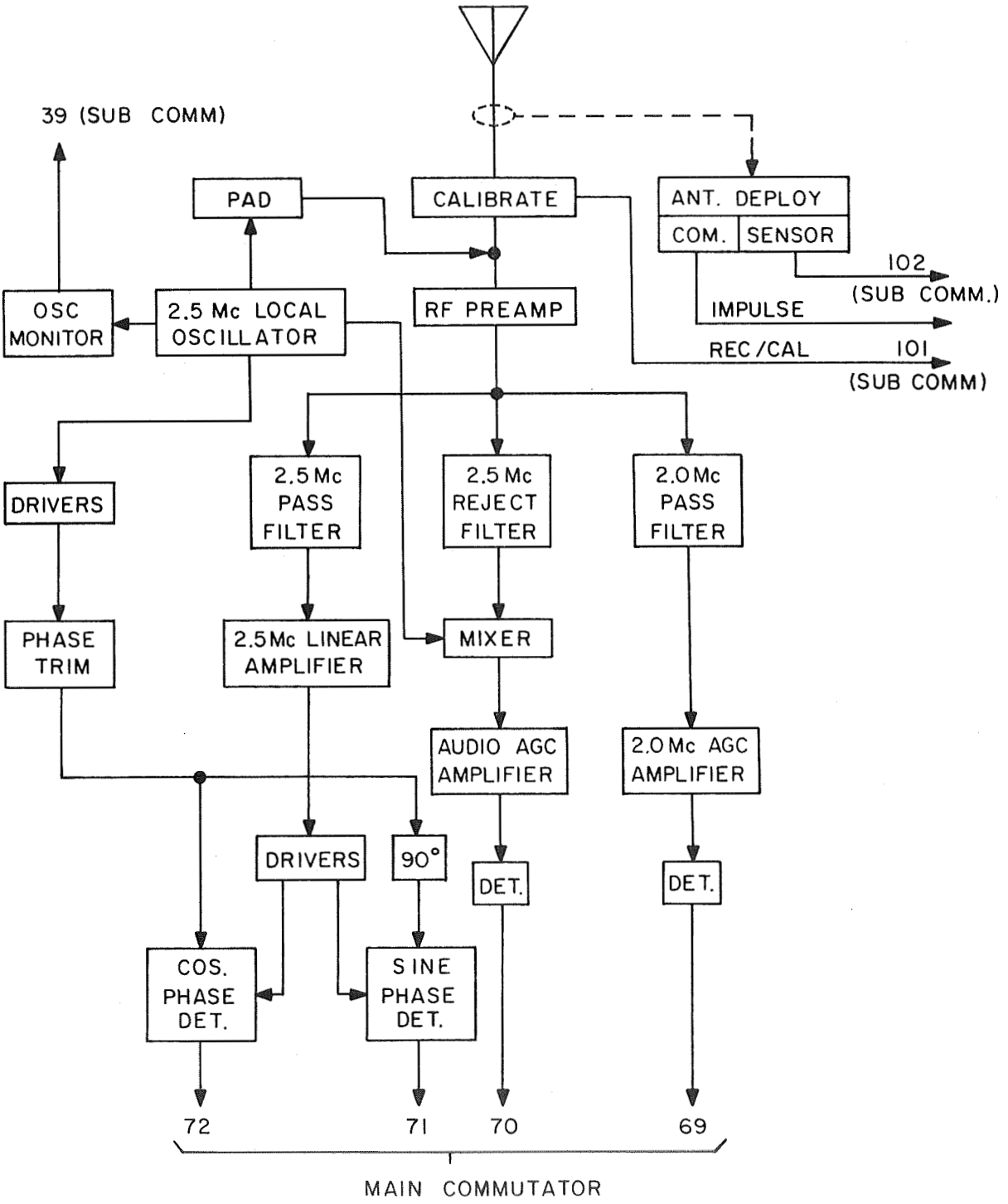

Figure 5. Block Diagram of the Experiment Package.

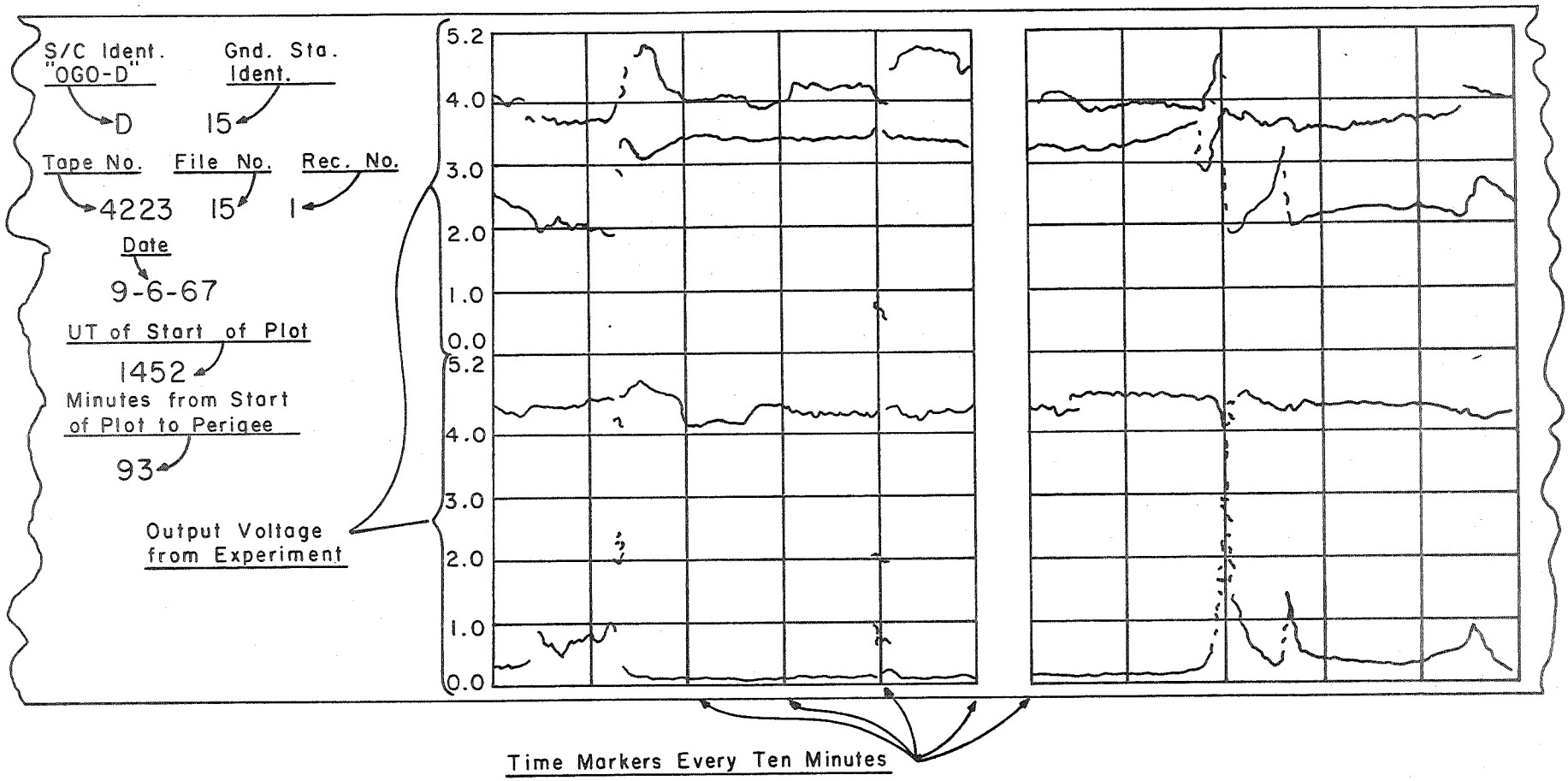

Figure 6. Format of the Plots of Unreduced OGO-IV Data on 35mm Film

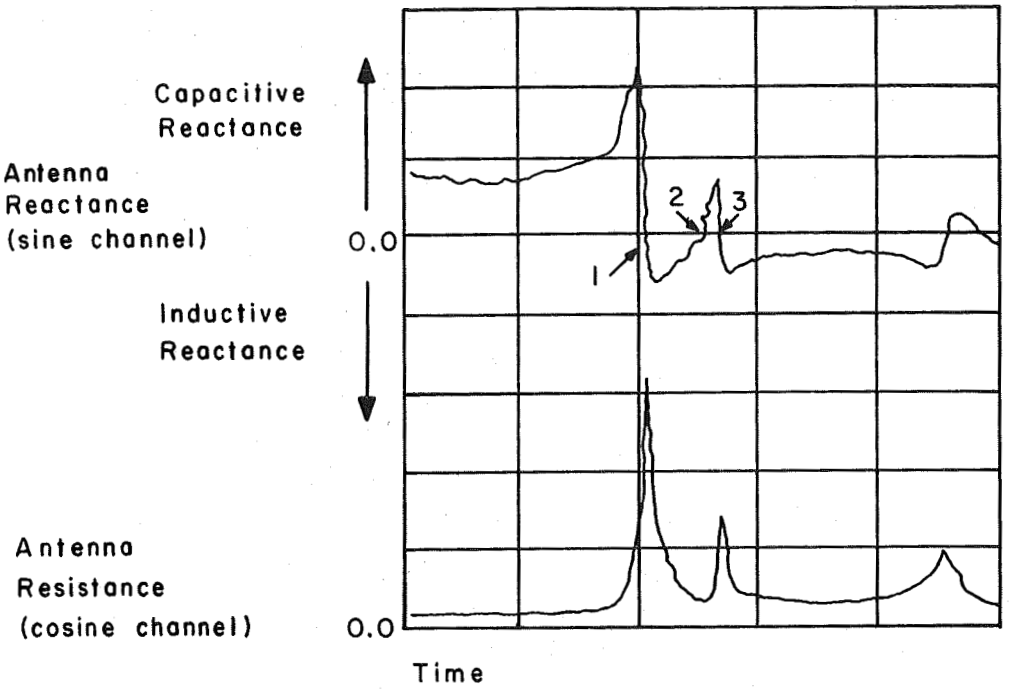

Figure 7. Measured Antenna Impedance as a Function of Time.

The points labeled 1, 2, and 3 are the first, second, and third sign changes in the reactive component, respectively.

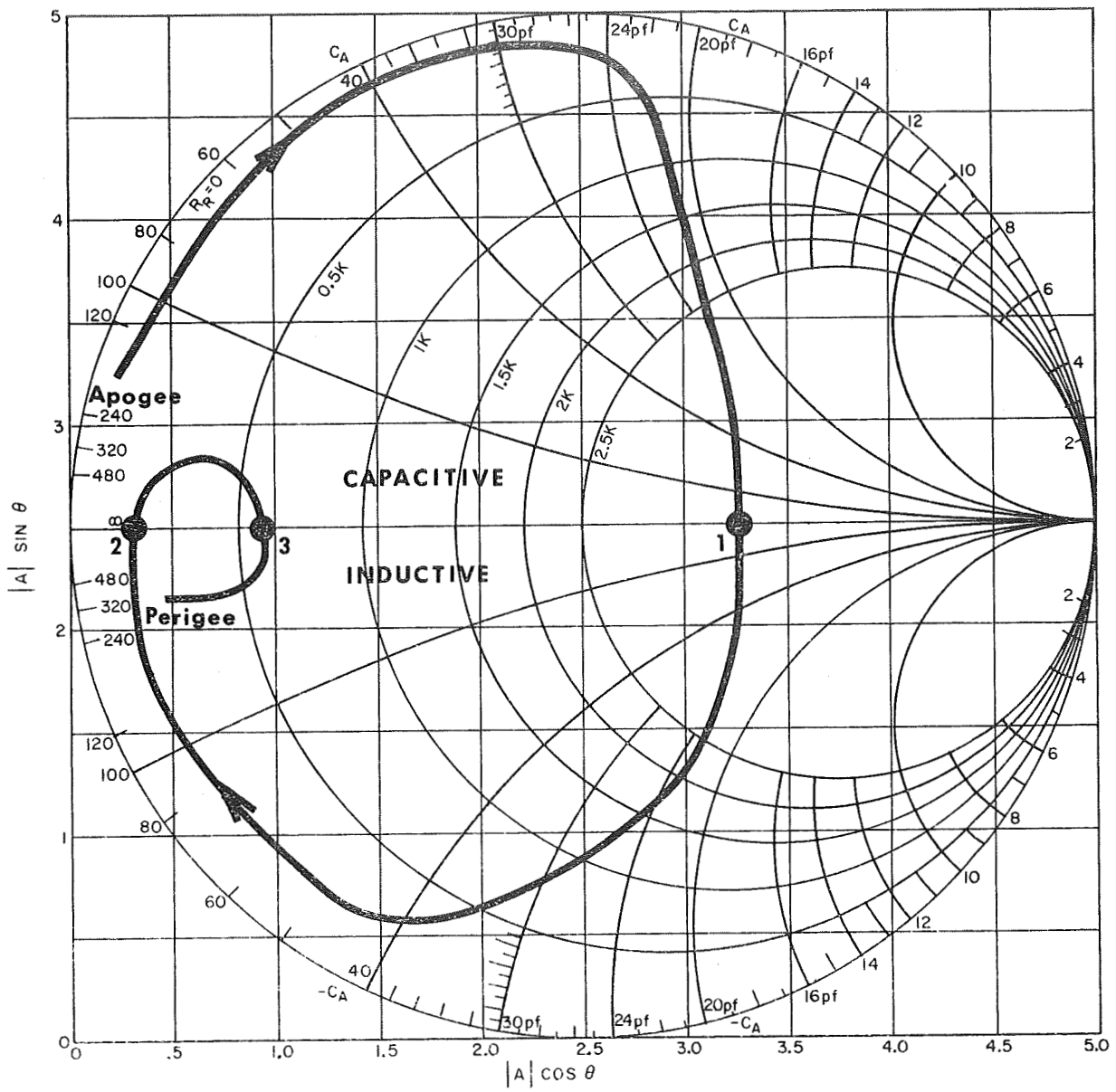

Figure 8. Smith Chart Trajectory of Antenna Impedance for a Typical OGO-IV Orbit.

The points labeled 1, 2, and 3 are the first, second, and third sign changes in the reactive component, respectively.

APPENDIX A
ILLUSTRATIVE SAMPLES OF DATA

Experiment data for two typical "good" passages through the ionosphere are presented as illustrative examples. "Good" passages are those for which there is no evidence of significant telemetry errors, no evidence of unusual interference to the radiometer channels, and no evidence of small-scale irregularities in the ionosphere, as evidenced by irregularities in the antenna impedance channels.

The two intervals are designated GI 3, where passage through the focussing region occurred about 0608 UT, August 5, 1967, and GI 8 at about 1859 UT, August 15, 1967.

The observed data which are plotted here include the data from the two radiometer channels at 2.0 and 2.5 MHz respectively, reduced to units of mean square noise voltage at the radiometer input, and the resistive and reactive components of antenna impedance, reduced to units of ohms. The geo-magnetic and geographic latitudes of the sub-satellite point are also plotted.

From these observed data and from the magnitude of the ambient magnetic field given in the attitude-orbit tape, the approximate plasma frequency and the ionospheric parameters $X = (f_p/f)^2$ and $Y = f_g/f$ are computed and plotted. The scales for X, Y, and Y^2 are so chosen that the points $X = 1-Y$, $X = 1-Y^2$, $X = 1$, and $X = 1 + Y$ are all readily identifiable.

In this example, a crude method has been used to deduce the plasma frequency, f_p, from the observed data. The point in time where the antenna reactance changes from capacitive

(negative) to inductive (positive) is the point where $X = 1 - Y^2$. Knowing Y, we may compute X and f_p at this point. Thus we have one reliable point on the curve $f_p(t)$. The point in time where the E-mode propagation disappears corresponds to $X = 1-Y$. If we identify the E-mode disappearance in each of the radiometer channels, we could determine two more points on the $f_p(t)$ curve. Unfortunately, the E-mode disappearance points are not readily identifiable in the radiometer data. But if we arbitrarily choose a point somewhere on the slope of the 2.5 MHz radiometer curve, and the corresponding point on the 2.0 MHz radiometer curve, we can perhaps obtain a reasonably good approximation to the slope of the $f_p(t)$ curve. We then draw a line through the one reliable point, using the slope determining from the two unreliable, but hopefully consistent, points. Figures A-2 and A-4 illustrate this operation. Here, the one reliable point, determined from the 2.5 MHz impedance channel, is plotted as a circled cross, and the two E-mode disappearance points are plotted as plain crosses. A straight line has been assumed for $f_p(t)$, though perhaps an exponential would be preferred. In any event, it is not safe to extrapolate very far from the one reliable point.

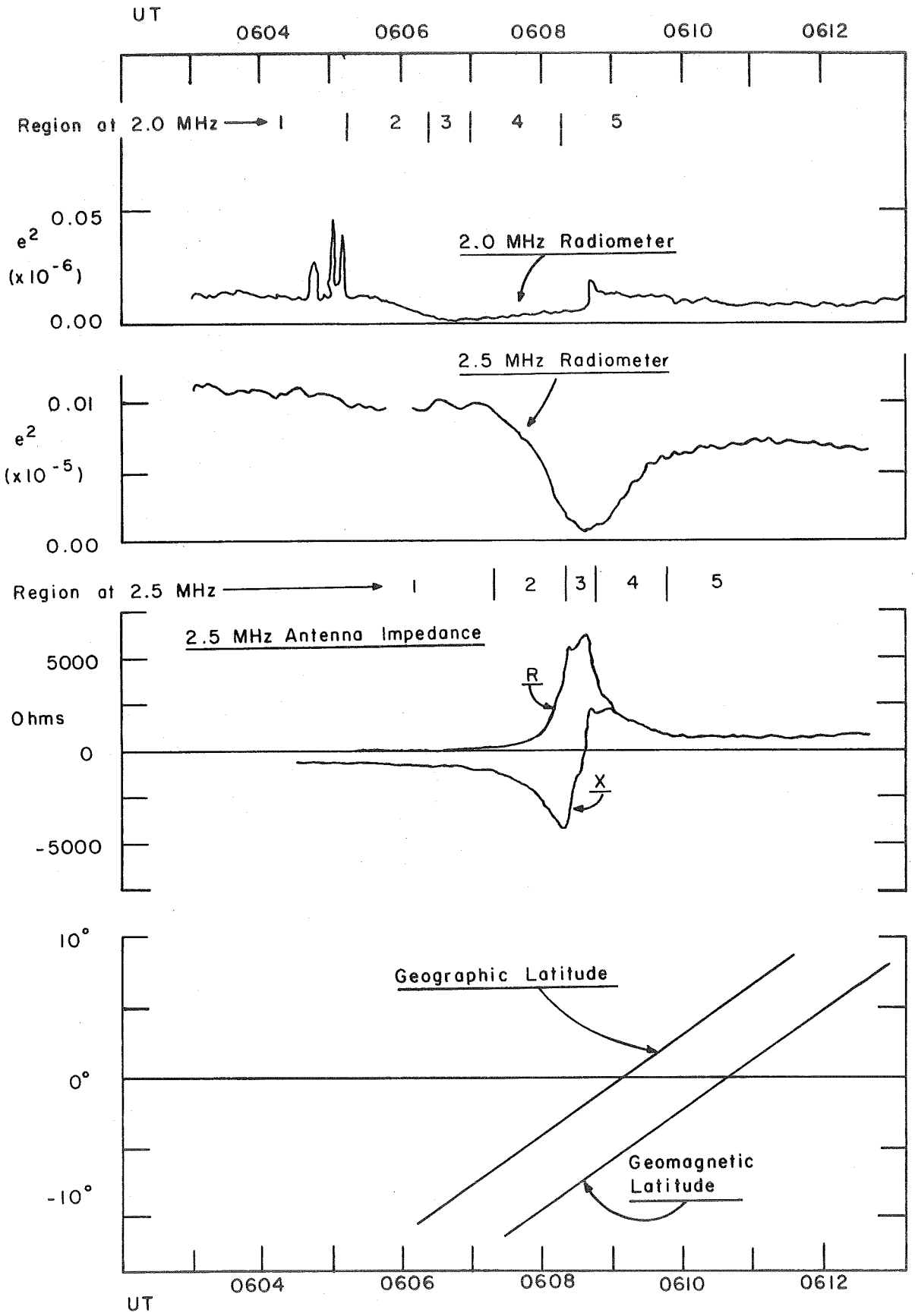

Figure A-1. Observed Data for OGO-IV Passage GI 3, 0608 UT, Aug 5, 1967.

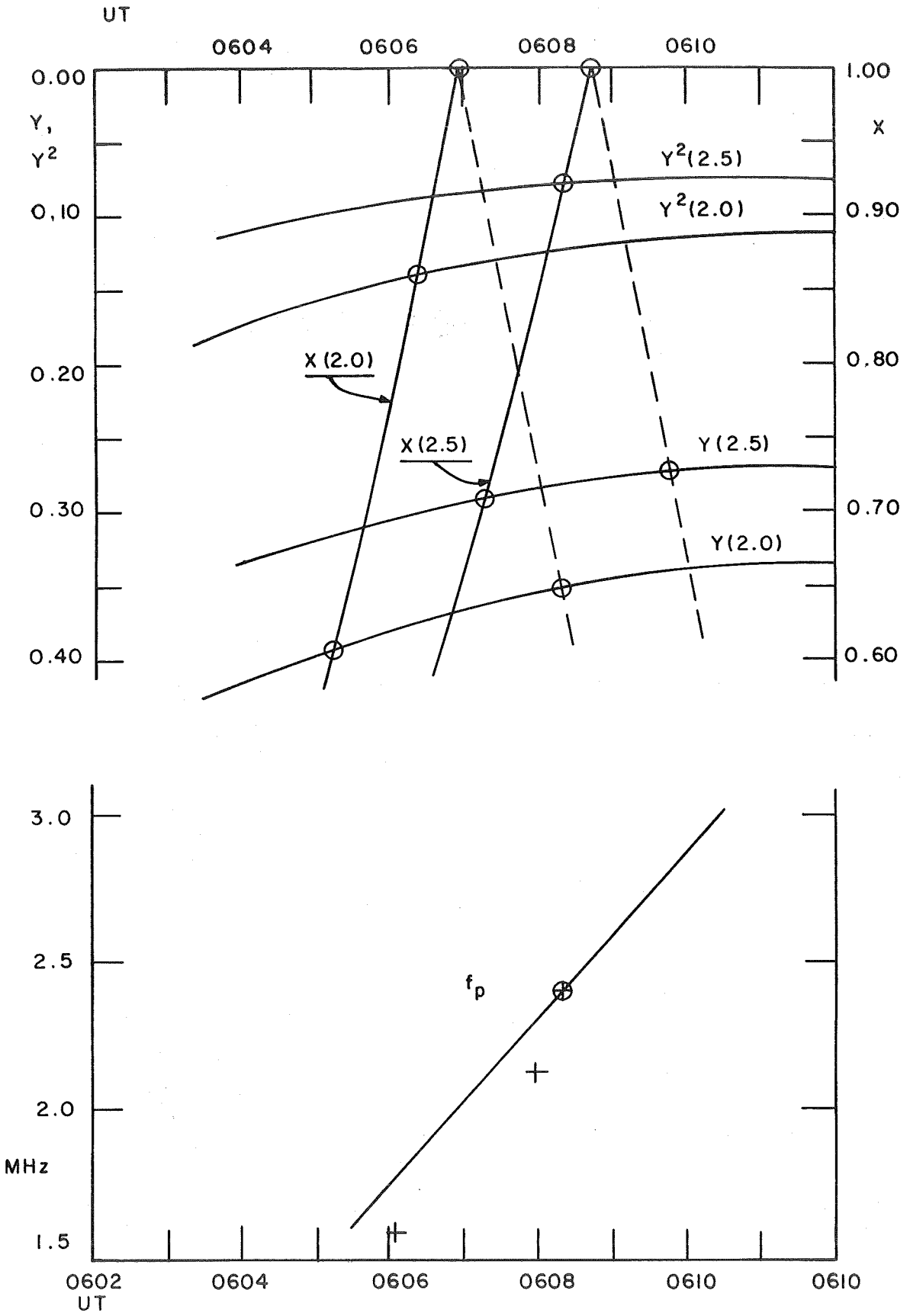

Figure A-2. Deduced Ionospheric Parameters for OGO-IV Passage GI 3, 0608 UT, Aug 5, 1967.

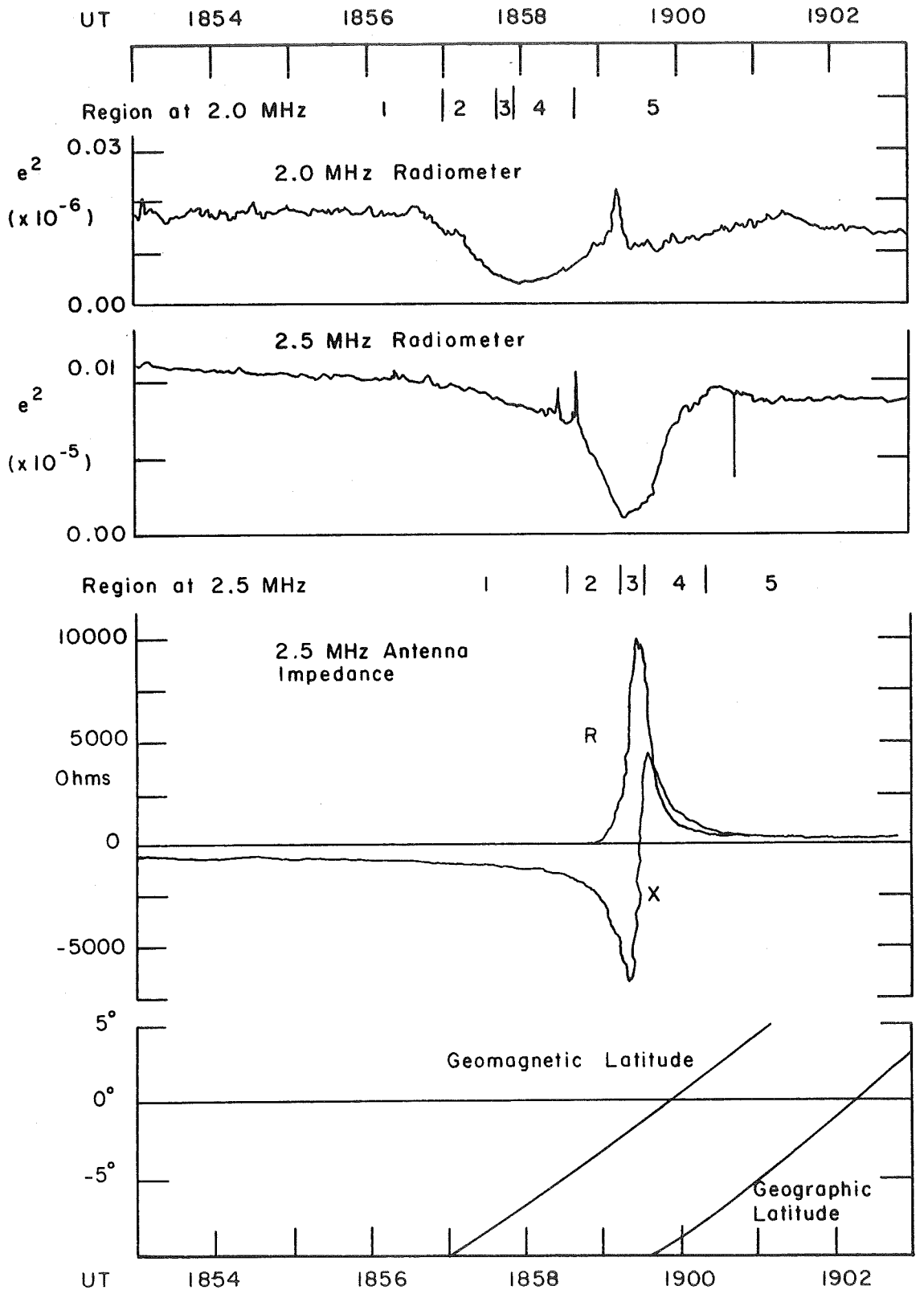

Figure A-3. Observed Data for OGO-IV Passage GI 8, 1858 UT, Aug 15, 1967.

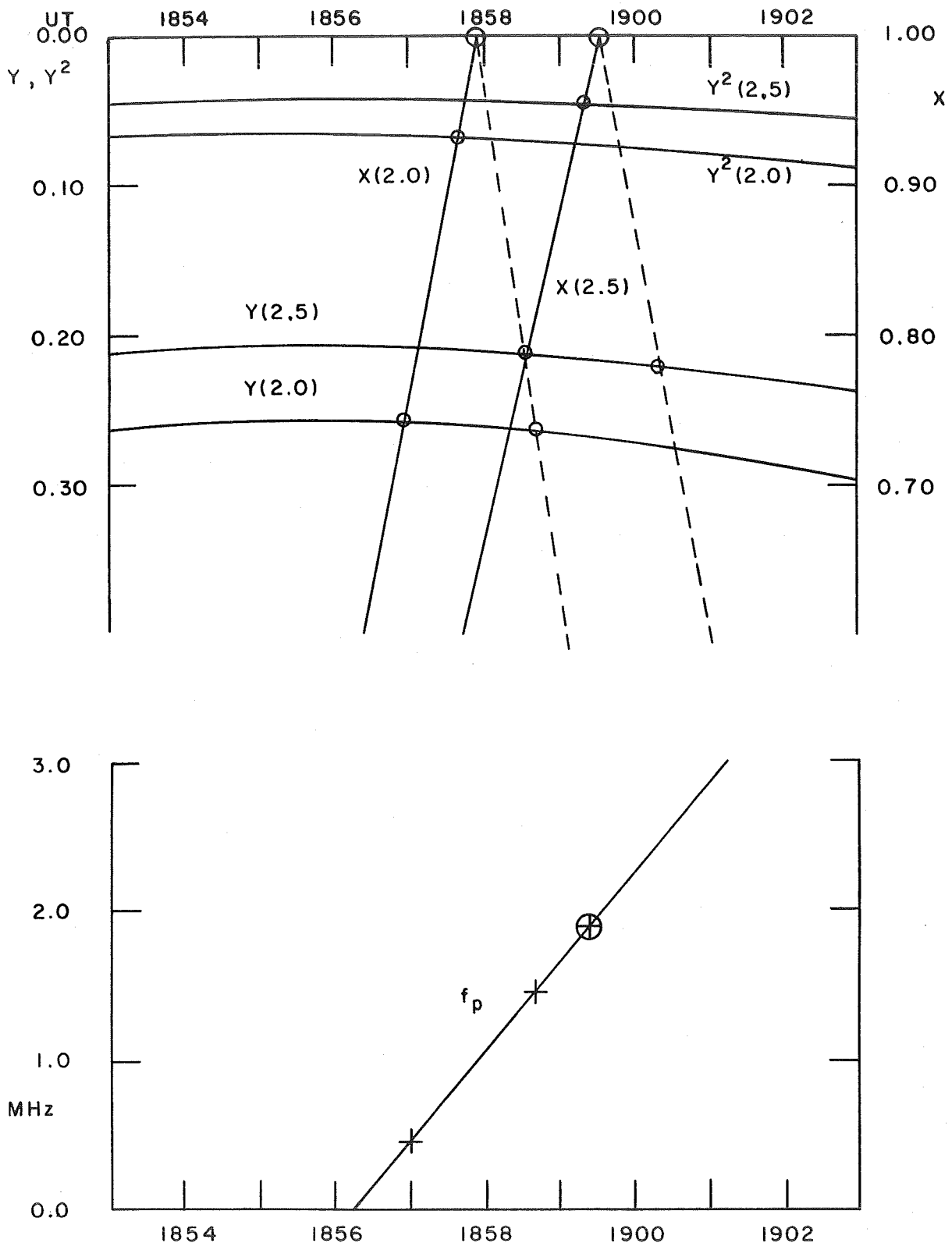

Figure A-4. Deduced Ionospheric Parameters for OGO-IV Passage GI 8, 1858 UT, Aug 15, 1967.

APPENDIX B

FORMAT FOR PROCESSED DATA TAPES

The output from the Part 2 program is stored in binary form on magnetic tape. The records contain both integers and floating point numbers of the following form:

INTEGER - one 24 bit word

FLOATING POINT - two 24 bit words, m and m+1, where

word m:	bits 0 - 14:	low order bits of the fraction
	bit 15:	sign of the exponent
	bit 16 - 23:	exponent.
word m+1:	bit 0:	sign of the fraction
	bits 1 - 23:	high order bits of the fraction

The output tapes are written by a FORTRAN II calling program on an SDS 930 computer.

Each file of data contains identifying information as well as experiment words from the POGO radiometer and impedance channels. Approximately twenty minutes of data is contained in each file. The records within a file will now be described.

Record 1 - six integers;

- word 1 - satellite ID; = 2 for OGO-II, and = 4 for OGO-IV
- word 2 - station number
- word 3 - UM/RAO input tape number
- word 4 - year
- word 5 - month
- word 6 - day

} of the data which follows

Record 2 - The label record from the Goddard Space Flight Center (GSFC) data tapes which contain 120 6-bit BCD characters in the format shown below (even parity).

Record 3 - 128 time words expressed as seconds of the day ($TIME_i$)

Record 4 - 128 values of R_A (RA_i)

Record 5 - 128 values of X_A (XA_i)

Record 6 - 128 values of V_L^2 for 2.0 MHz ($V2L20_i$)

Record 7 - 128 values of V_L^2 for 2.5 MHz ($V2L25_i$)

} all floating point words

The word $TIME_1$ is the time associated with RA_1, XA_1, $V2L20_1$, $V2L25_1$.

Record 8-end - repeats records 3-7 for each 31.232 seconds of time until the end of the selected interval.

A file mark ends the data for one selected interval.

Label (ID) Record for S-50, Master Binary Tape and All Experimenters Decom Tapes

The first record per file is called the Label Record. It serves as a means to identify the data contained on that file of which it is a part. Each record will contain 120 six-bit characters in a form suitable for direct printing.

The format of the Label Record is as follows:

CHARACTER	REPRESENTATION
1 - 5 + Space	Satellite Identification (assigned after launch) Example: 65021 where: 65 = year of launch 02 = Beta 1 = object
7 - 8 + Space	Year
10 - 12 + Space	Station Number Example 001 = Blossom Point 020 = Rosman
14 - 15 + Space	Analog File Number
17 - 20 + Space	Analog Tape Number
22 - 23 + Space	Buffer File Number
25 - 28 + Space	Buffer Tape Number
30 - 32 + Space	Date of data digitization (day of year)

CHARACTER	REPRESENTATION
34 - 66	Will be identical to characters 1 - 33 unless an error was found in those characters. If that is the case, then this portion of the record will contain the corrected values of that field.
67 + Space	Type of data contained in file 0 = 4 kilobit real time 1 = 16 kilobit real time 2 = 64 kilobit real time 3 = command storage playback
69 - 71 + Space 73 - 77 + Space	Day of year Seconds of day start time of data
79 + Space	Is Flexible Format in use? 1 = yes 0 = no
81 - 82	Flexible Format Number
83 - 88	Blank
89 + Space	Equipment Group in use (1 or 2)
91 - 94 + Space	Master Binary Tape Number
96 - 97 + Space	Master Binary File Number
99 - 100 + Space 102 - 103	A/D line operator ID AD/line ID
104 - 113	Blank
114 - 115	Reel Sequence Number
116 - 118	Run Number
119 - 120	Experiment Number

APPENDIX C
DESCRIPTION OF DATA FACILITY

The data facility of the University of Michigan Radio Astronomy Observatory consists of an SDS-930 computer, and a special buffer-display system, designed and built by the staff. Software is based upon the SDS MONARCH system, supplemented by locally written subroutines for handling the special equipment.

The computer has a core memory capacity of eight thousand words, of twenty-four bits each, backed up by a disc of 250,000 words. It is provided with a real time clock, sixteen priority interrupts, twenty-four special output lines (set lines), setable by program, and twenty-four special input lines (sense lines), whose state can be sensed by the program. The I/0 devices on the computer are a teletype, card reader, high-speed line printer, and two seven-track magnetic units.

The special buffer-display system, designed and built by RAO personnel, includes a buffer core memory of four thousand words of thirty-six bits each, controlled by a stored-program I/0 channel. I/0 devices presently connected to the buffer-display system include a direct-view CRT display, a photographic CRT display with an automatic 35mm camera, an incremental plotter, an input keyboard, an analog-to-digital converter, and a magnetic tape unit. The I/0 channel of the buffer-display system can transfer data between the buffer core and the computer, as well as between the buffer core and its own I/0 devices, so the system can be used either in an on-line or off-line mode.

A "user's console," associated with the display unit, permits the user to communicate control decisions back to the computer. Thus the system provides for complete interaction between the user and the computer, via the display and user's console.

Special software, written by the UM/RAO staff, permits the entire system to be used by the FORTRAN programmer. Library subroutines provide for graphic output on the direct view CRT, the photographic CRT, and the incremental plotter. Other subroutines permit the program to react to the push-buttons, switches, and the "joystick" control on the user's console.

Two special off-line data facilities designed and built by the UM/RAO staff are the data logger and the tape-to-film converter. The data logger includes a fourteen-bit analog-to-digital converter and a sixteen channel multiplexer. Its function is to convert analog voltage signals to digital form, and record them on computer-compatible magnetic tape. The tape-to-film converter includes a small CRT display and a 35mm camera. Its function is to accept data on digital magnetic tape, and to generate intensity-modulated plots on film. Both of these units are in the process of being absorbed into the main data system.

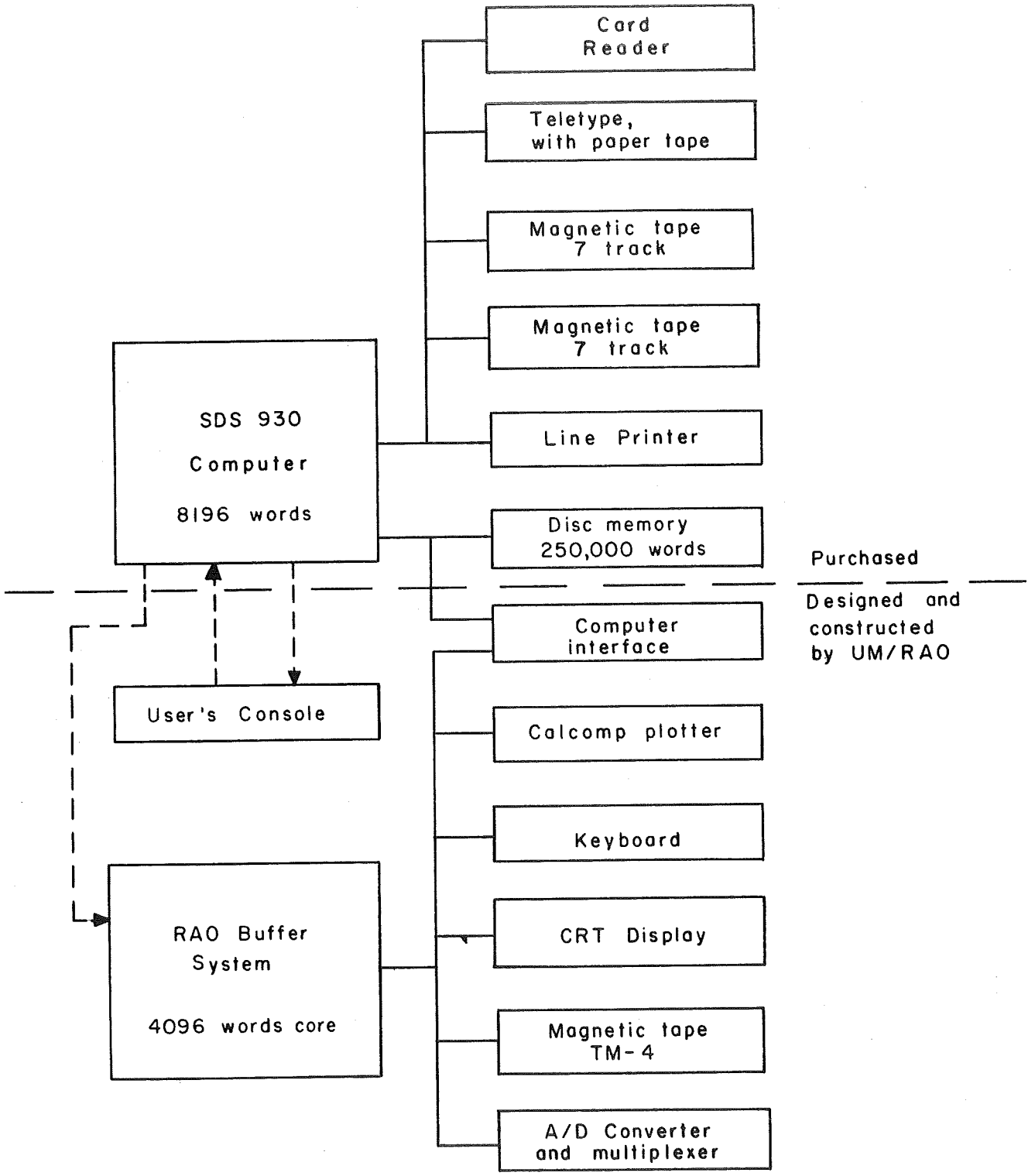

Figure C-1. Block Diagram of the UM/RAO Data Processing Facility